Universidade do Minho
Escola de Medicina

Hugo Miguel Fernandes Silva

Metabolic biomarkers of chick embryonic lung development: impact of retinoic acid

Biomarcadores metabólicos do pulmão embrionário de galinha em desenvolvimento: impacto do ácido retinoico

setembro de 2017

Hugo Miguel Fernandes Silva **Metabolic biomarkers of chick embryonic lung development: impact of retinoic acid**

UMinho | 2017

Universidade do Minho
Escola de Medicina

Hugo Miguel Fernandes Silva

Metabolic biomarkers of chick embryonic lung development: impact of retinoic acid

Biomarcadores metabólicos do pulmão embrionário de galinha em desenvolvimento: impacto do ácido retinoico

Dissertação de Mestrado
Mestrado em Ciências da Saúde

Trabalho efetuado sob a orientação da
Doutora Rute Carina Silva Moura
e do
Professor Doutor Jorge Manuel Nunes Correia Pinto

setembro de 2017

"Equipped with his five senses, man explores the universe around him and calls the adventure: Science"

Edwin Powell Hubble
The Nature of Science

ACKNOWLEDGEMENTS

Quero expressar os meus sinceros agradecimentos a todas as pessoas e instituições que, de uma forma mais ou menos direta, contribuíram para a elaboração desta tese de mestrado e conclusão desta etapa académica. Primeiramente gostaria de agradecer à instituição Universidade do Minho e em particular à Escola de Medicina e ao Instituto de Investigação em Ciências da Vida e Saúde (ICVS) por me receberem para realização do mestrado e do trabalho prático referente a esta tese. Agradeço especialmente ao laboratório I1.03, Domínio das Ciências Cirúrgicas pela cedência do espaço. Agradeço também ao laboratório de Biologia Celular, Departamento de Microscopia, Instituto de Ciências Biomédicas Abel Salazar (ICBAS), Universidade do Porto, pela disponibilidade e espaço laboratorial que me permitiram realizar algumas das tarefas práticas. Gostaria de agradecer à Doutora Rute Moura, ao Doutor Marco Alves e ao Doutor Pedro Oliveira pela orientação durante todo este trabalho. Agradeço por toda a paciência, compreensão, apoio, motivação, conselhos e ensinamentos que, decididamente, contribuíram para a minha evolução pessoal e profissional, ao longo deste percurso. Ao Professor Doutor Jorge Correia Pinto por todo o apoio.

Agradeço a toda equipa laboratorial I1.03: Tiago, Violina, Henrique, Marta, Gonçalo, Patrícia Cunha, Carla Gonçalves, Ana Gonçalves, Patrícia Terra, Caroline, Catarina, Sofia e Sandra Costa por todo o companheirismo, motivação e constante troca e discussão de ideias.

Agradeço a toda a equipa do Porto: Tânia, Raquel, Maria João, Ana Martins, Susana, João Monteiro, Bruno, David, Bernardo, Luís Crisóstomo, Luís Rato, Rute e Tatiana pelo companheirismo, pelo grande espírito de equipa e pela interajuda.

Ao Tiago por todo o apoio, troca de ideias e pela sua energia contagiante.

Ao Henrique e à Marta pelo companheirismo e motivação dada ao longo dos 2 meses.

Ao David, um verdadeiro companheiro de luta, obrigado por tudo.

Ao Luís Crisóstomo, pela partilha da sua experiência, por todas as aulas de estatística, pelas trocas de ideias e pelas discussões científicas.

À Maria João, que desde o início não hesitou em ajudar. Pela motivação, compreensão, conselhos e ensinamentos. Pela "garra" contagiante com que trabalha diariamente.

Aos amigos de sempre, pelo apoio incondicional, companheirismo e motivação.

Aos meus pais, à minha irmã e à restante família, por todo o apoio incondicional ao longo do meu percurso, motivando-me e dando-me força para continuar e atingir todas as minhas metas.

The work presented in this dissertation was performed at the Surgical Sciences Research Domain of the Life and Health Sciences Research Institute (ICVS), School of Medicine, University of Minho, Braga, Portugal (ICVS/3B's – PT Government Associate Laboratory, Braga/Guimarães, Portugal). The work was supported by FEDER funds, through the Competitiveness Factors Operational Programme (COMPETE), and by National funds, through the Foundation for Science and Technology (FCT), under the scope of the Project POCI-01-0145-FEDER-007038; and by the Project NORTE-01-0145-FEDER-000013, supported by the Northern Portugal Regional Operational Programme (NORTE 2020), under the Portugal 2020 Partnership Agreement, through the European Regional Development Fund (FEDER).

ABSTRACT

Pulmonary development is a complex process that depends on the activation of conserved signaling pathways that regulate cellular processes such as proliferation, differentiation and migration. Retinoic acid (RA) signaling is one of the active pathways during lung organogenesis, since it modulates branching morphogenesis in a dose-dependent manner. It is widely accepted that the cellular events underlying embryonic development require high amounts of energy and nutrients to form new biomass. However, the metabolic changes that occur during lung branching morphogenesis have not been described so far. In this work, we have characterized, for the first time, the metabolic profile of chick lung branching in early stages of development: b1, b2 and b3 (1, 2 or 3 secondary bronchi, respectively). Furthermore, the impact of RA on lung branching metabolism was evaluated. *Ex vivo* lung explant culture was performed in the presence or absence of RA, and the medium collected to analyze the production/consumption of metabolites associated with glucose catabolism (glucose, lactate, acetate, alanine), by ^{1}H-NMR. qRT-PCR and *in situ* hybridization were performed to assess the expression levels and patterns of key enzymes and transporters from glucose catabolic pathway. In normal conditions, the major metabolite variations occur from stage b1 to stage b3. In b3, there is an increase in lactate and acetate production. Still, glucose consumption is maintained from b1 to b3 stage with a concurrent decrease of glucose transporter 3 (*glut3*) transcript levels, and a decrease in hexokinase 1 (*hk1*) levels in b3 stage. This phenomenon suggests an increase in the glycolytic efficiency and a shift to lactate production. In fact, we observed a decrease on pyruvate dehydrogenase B (*pdhb*) and an increase in lactate dehydrogenase A (*ldha*) expression levels in b3 stage, while lactate dehydrogenase B (*ldhb*) levels decrease. Embryonic lung expression pattern of *glut3*, *hk1*, *ldha*, *ldhb* and *pdha* were characterized suggesting hypothetical interactions between the mesenchymal and epithelial compartments. When b2 lung explants were exposed to RA, glucose consumption, alanine and lactate production decreased. On the other hand, glutamate, glutamine consumption, and acetate production remain unaltered whereas pyruvate production increased. This phenomenon is accompanied by an increase in *ldha* expression levels. This study describes, for the first time, the temporal metabolic changes associated with chick pulmonary branching. It seems that glycolytic efficiency is increased, with a concurrent metabolic shift from Krebs cycle to lactate production. Furthermore, acetate and lactate are potentially seen as metabolic biomarkers of lung development. On the other hand, RA triggers a metabolic shift where lipids may be potentially seen as source of carbons and energy during RA-induced branching morphogenesis.

RESUMO

O desenvolvimento pulmonar é um processo complexo que depende da ativação de vias de sinalização conservadas que regulam diversos processos celulares, nomeadamente proliferação, diferenciação e migração. A via de sinalização do ácido retinoico é uma das vias cruciais na morfogénese pulmonar uma vez que modula a ramificação pulmonar. Sabe-se que durante o desenvolvimento embrionário são necessárias elevadas quantidades de energia e nutrientes para formação de biomassa. No entanto, as alterações metabólicas que ocorrem ao longo do processo de ramificação pulmonar ainda não foram descritas. Neste trabalho, caracterizamos, pela primeira vez, o perfil metabólico da ramificação pulmonar de galinha, em estadios precoces do desenvolvimento: b1, b2 e b3 (1, 2 ou 3 brônquios secundários, respetivamente). Adicionalmente, descrevemos o impacto do ácido retinoico sobre o metabolismo durante a ramificação pulmonar. Realizaram-se cultura de explantes pulmonares em condições normais e na presença de ácido retinoico; os meios de cultura foram analisados, por ^{1}H-NMR, para determinar a produção/consumo de metabolitos associados ao catabolismo da glucose (glucose, lactato, acetato, alanina). O padrão e os níveis expressão de transcritos de enzimas e transportadores implicados no catabolismo da glucose foram analisados por hibridização *in situ* e qRT-PCR, respetivamente. O padrão de expressão de *glut3*, *hk1*, *ldha*, *ldhb* e *pdha* sugere potenciais interações entre o mesênquima e epitélio pulmonar. A nível de metabolitos, as maiores variações ocorrem entre o estadio b1 e o estadio b3, em condições normais. Em b3, há um aumento da produção de lactato e acetato. No entanto, o consumo de glucose mantém-se de b1 para b3, havendo uma diminuição dos níveis de expressão do transportador de glucose 3 (*glut3*) e da hexoquinase 1 (*hk1*) em b3. Este fenómeno sugere um aumento da eficiência glicolítica e uma alteração para um metabolismo que resulta na produção de lactato. Na verdade, verifica-se uma diminuição dos níveis de expressão da piruvato desidrogenase B (*pdhb*) e aumento dos níveis de expressão da lactato desidrogenase A (*ldha*) no estadio b3, enquanto que os níveis de lactato desidrogenase B (*ldhb*) diminuem. Quando explantes de pulmões b2 foram expostos, *in vitro*, a ácido retinoico, o consumo de glucose e produção de alanina e lactato diminuíram. Por outro lado, o consumo de glutamato e de glutamina, bem como a produção de acetato permaneceram inalterados, com um aumento da produção de piruvato. Este fenómeno foi acompanhado por um aumento da expressão de *ldha*. Neste estudo, são descritas, pela primeira vez, as alterações metabólicas que ocorrem ao longo do tempo, associadas ao processo de ramificação pulmonar de galinha. Durante o processo, a eficiência glicolítica está aumentada e parece haver uma alteração do metabolismo baseado no ciclo de Krebs para

o metabolismo de produção de lactato. Assim, o acetato e o lactato são potencialmente biomarcadores do processo de desenvolvimento pulmonar. Por outro lado, o ácido retinoico estimula uma alteração metabólica sendo que os lipídios surgem como fonte de carbono e energia plausível que acompanha a ramificação pulmonar induzida pelo ácido retinoico.

TABLE OF CONTENTS

FIGURE INDEX

TABLE INDEX

Abbreviation List

^{1}H-NMR – ^{1}H Nuclear Magnetic Resonance

ADH – Alcohol Dehydrogenase

BCIP – 5-Bromo-4-Chloro-3-Indolyl Phosphate

BCMO – β-carotene-15, 15'-Monooxygenase

BMP – Bone Morphogenetic Protein

BPD – Bronchopulmonary Dysplasia

CCAM – Congenital Cystic Adenomatoid Malformation

CDH – Congenital Diaphragmatic Hernia

cDNA – Complementary DNA

CRABP – Cellular Retinoic Acid-binding Protein

CYP26 – Cytochrome P450, Family 26

DGTA1 – Diacylglycerol O-acyltransferase 1

DNA – Deoxyribonucleic Acid

EDTA – Ethylenediamine Tetraacetic Acid

EGTA – Ethylene Glycol Tetraacetic Acid

FGF – Fibroblast Growth Factor

GSK – Glucokinase

HAT – Histone Acetylase

HDAC – Histone Deacetylase

HH – Hamburger and Hamilton Developmental Table

HSCs – Hepatic Stellate Cells

LB – Luria Bertani Medium

LP – Pancreatic Lipase

LRAT – Lecithin Retinol Acyltransferase

MABT – Maleic Acid Buffer with Tween 20

mRNA – Messenger RNA

NADH – Nicotinamide Adenine Dinucleotide

NADPH – Nicotinamide Adenine Dinucleotide Phosphate

NBT – 4-Nitro Blue Tetrazolium Chloride

NCOA – Nuclear Receptor Co-activators

NCOR – Nuclear Receptor Co-repressors

PBS – Phosphate Buffered Saline

PBT – Phosphate Buffered Saline with Tween 20

PCK – Phosphoenolpyruvate Carboxykinase

PCR – Polymerase Chain Reaction

PPARγ – Peroxisome Proliferator-activated Receptor γ

ppm – Parts Per Million

PRC2 – Polycomb Repressive Complex 2

qRT-PCR – Quantitative Polymerase Chain Reaction

RA – Retinoic Acid

RALDH – Retinaldehyde Dehydrogenase

RAR – Retinoic Acid Receptor

RARE – Retinoic Acid Response Element

RBP – Plasma Retinol-binding Protein

RDH – Retinol Dehydrogenase

RE – Retinyl Esterase

RNA – Ribonucleic Acid

RXR – Retinoic X Receptor

SCARB – Scavenger Receptor, class B

SHH – Sonic Hedgehog

STRA6 – Stimulated by Retinoic Acid 6

TCA – Tricarboxylic Acid Cycle

TEF – Tracheal-Esophageal Fistula

TGFβ – Transforming Growth Factor βeta

VAD – Vitamin A Deficiency

WNT – Wingless-related Integration Site

1. INTRODUCTION

1.1 The Respiratory System: Overview

The respiratory system is composed by the trachea, lungs and the associated vasculature. This system is adapted to the terrestrial life, and it is primarily responsible for gas-exchange, providing an intimate contact between the atmosphere and the circulatory system. All through the highly branched pulmonary structure the air is cleaned, humidified and is able to reach the blood vessels. In fact, lungs are directly exposed to the external environment and, therefore, are continuously exposed to temperature fluctuations, humidity variations, particulate matter, allergens, and harmful substances from pollution, among many potential external injuries (Herriges & Morrisey, 2014). To survive to these damaging conditions, the respiratory system developed compensatory mechanisms at the cellular level, which are responsible for re-stablishing the correct homeostasis. Accordingly, several signaling cascades are constantly communicating and regulating each other to trigger the correct physiological responses; nevertheless, occasionally, these mechanisms are not adequately efficient and permanent damage settles inducing disease. Conversely, when damage occurs during early embryonic development, congenital malformations may cause lung abnormalities such as Tracheal-Esophageal Fistula (TEF), Congenital Cystic Adenomatoid Malformation (CCAM), Bronchopulmonary Dysplasia (BPD) and Congenital Diaphragmatic Hernia (CDH), just to mention a few (Balkissoon et al., 2011; Davidson & Berkelhamer, 2017). Congenital lung diseases display high morbidity and mortality rates and for this reason it is imperative to explore and better understand the etiology of these particular disorders (Keller et al., 2010; Nogueira-Silva et al., 2011). In this context, it is crucial to understand the molecular mechanisms underlying normal lung development to better comprehend what induces disease and, eventually, establish or suggest therapeutic strategies.

1.2 Lung Development

Lung development is a very complex process governed by epithelium-mesenchyme interactions, and regulated by several transcription and growth factors which, together, contribute to the correct formation of the organ. Lung is constituted by two different cellular compartments. The epithelial compartment which arises from the endoderm layer and later gives rise to all the lung branching-like structure, and the mesenchymal compartment that originates from mesoderm and gives rise to the lung connective tissue, smooth muscle, endothelial cell precursors, the cartilage rings of the trachea and the mesothelial cells that originate the pleura (Herriges & Morrisey, 2014). Several signaling cascades,

operating in both epithelial and mesenchymal compartment, need to be activated precisely in time and space to ensure proper lung development, among them: FGF (Fibroblast Growth Factor), SHH (Sonic Hedgehog), TGFβ-BMP (Transforming Growth Factor β-Bone Morphogenetic Protein), WNT (Wingless-related Integration Site), NOTCH and RA (Retinoic Acid) (Warburton et al., 2005; Cardoso & Lu, 2006; Morrisey & Hogan, 2010; Ornitz & Ying, 2012).

1.2.1 Mammalian Lung Development

In mammals, the respiratory system arises from the ventral foregut endoderm, where specification of the lung cell fate occurs (Morrisey & Hogan, 2010). These cells differentiate and proliferate giving rise to the laryngotracheal groove (Kimura & Deutsch, 2007). From this primitive structure, the trachea emerges, at the proximal level, and the lung starts to appear in the distal region, around mouse embryonic day 9.5 (E9.5). Next, primary buds appear and, simultaneously, the separation of two tubular structures leaning against each other initiates, originating the esophagus and the trachea (Morrisey & Hogan, 2010, 2010). Lastly, the entire lung structure forms from successive branching of the epithelial tissue. The branching morphogenesis of the bronchi can be divided in three branching subroutines, according to the branching layout: domain branching, planar bifurcation and orthogonal bifurcation. Briefly, from the primary bronchus, secondary bronchi (buds) start to sprout and, on it turn, give origin to tertiary generation of buds (Warburton et al., 2005; Metzger et al., 2008; Warburton, 2008). With successive splitting and growth of the epithelium into the adjacent mesenchymal compartment, the mature airway tree develops and culminates with alveoli formation in the distal region of the lung (Warburton et al., 2010). Actually, lung development process can be divided into five embryonic stages according to major morphological and cellular events: embryonic, pseudoglandular, canalicular, saccular and alveolar. The embryonic and pseudoglandular, also known as early stages, are related with the establishment of the conducting airways; canalicular, saccular and alveolar, late phases, are more associated with the alveolar development, the vasculature formation, and the reduction of the mesenchymal compartment to form the thin air-blood interface that plays the crucial role of gas-exchange (Kimura & Deutsch, 2007; Herriges & Morrisey, 2014). The major stages of mammalian embryonic lung development are represented in Figure 1.

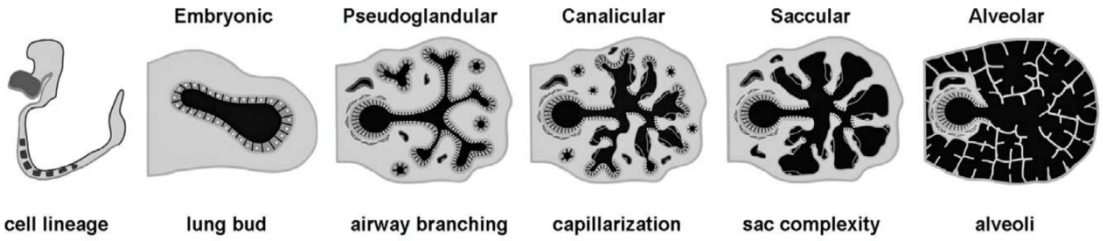

Figure 1 – Stages of Mammalian Lung Development. Embryonic: formation of primary lung buds and outgrowth from the ventral foregut. Pseudoglandular: airway branching. Canalicular: increase in capillary number. Saccular: formation of air sacs (primitive alveoli). Alveolar: formation of alveoli. Adapted from (Kimura & Deutsch, 2007).

1.2.2 Avian Lung Development

The avian respiratory system is constituted by the parabronchial lung and air sacs instead of alveoli. Together, both structures allow efficient gas-exchange and air movements in organisms with very high metabolic rates, such as birds (Bellairs & Osmond, 2014). The avian primordial lung appears at day 3.5 of embryogenesis as a protuberance, from the primitive foregut. From the same embryonic projection, the trachea and larynx structures emerge. The lung primordium leads to the development of the primary bronchus (mesobronchus) and later, due to lateral sprouting, to the secondary bronchi (Sakyama et al., 2003). During the course of this process, the mesobronchus grows distally and the number of new branches (secondary and tertiary) rapidly increase (Maina, 2003). Branching morphogenesis is defined by the process by which secondary bronchi sprout laterally into the surrounding mesenchyme compartment. Interestingly, this lateral or monopodial branching shows high similarity with the domain branching subroutine characteristic of the mammalian lung (Metzger et al., 2008; Kim et al., 2013). Lastly, air sacs are formed, culminating in a mature and well prepared respiratory system, able to ensure efficient gas-exchange.

1.2.3 Avian *vs* Mammalian Lung

Anatomically, in the adult stage, respiratory system of birds is quite different from mammals. The avian lung exhibits a parabronchial structure while the mammalian lung presents an airway tree structure (Maina, 2003; Metzger et al., 2008). In birds, air sacs pump the air through the stationary lungs so that oxygen is able to meet the capillary vessels, allowing gas-exchange. In opposition, in mammals, gas-exchange occurs in the alveolar structures localized in the terminal branches of the lung. The avian lung displays a unidirectional air flow that allows higher oxygen content inside the lungs; this feature is an advantage since it allows birds to extract enough oxygen, even at higher altitudes, where air is rarefied. On the other hand, mammals present a bidirectional air flow, which means that the fresh air is mixed

with residual air that remains in the lung after breathing, resulting in less content of oxygen, in comparison with birds. Despite all the differences in the adult stage, at early stages of lung development, the avian and mammalian lungs are quite similar in terms of structure, Figure 2.

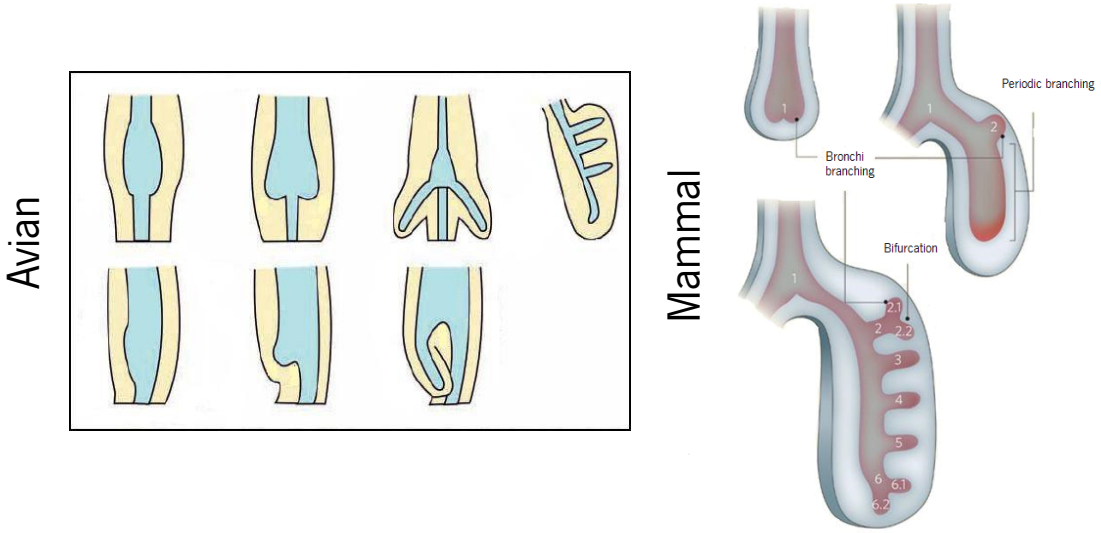

Figure 2 – Avian *versus* Mammalian Lung Development. Primary bronchus formation and branching morphogenesis with emergent secondary buds. The avian lateral/monopodial branching (left panel) shows high similarity with mammalian domain branching subroutine (right panel). Adapted from (Sakiyama et al., 2003; Warburton, 2008).

Furthermore, the molecular aspects underlying branching morphogenesis (pseudoglandular phase) seem to be highly conserved between these two species and point to, most probably, similar functions (Maina, 2012; Moura & Correia-Pinto, 2017). For instance, FGF signaling pathway is essential for chick primary bud formation and plays a critical role in branching morphogenesis (Sakyama et al., 2003; Moura et al., 2011). Similarly, SHH signaling pathway has been described as pivotal during early lung development, since its members are expressed in the chick embryonic lung (Moura et al., 2016). Moreover, WNT signaling cascade seem to be implicated not only in early branching stages (Moura et al., 2014) but also with vasculature development (Loscertales et al., 2008). Likewise, other essential cascades such as TGFβ-BMP and microRNAs are active in chick developing lung (Gleghorn et al., 2012; Moura et al., 2015). Recently, it has also been shown that RA regulates an intricate molecular network that contributes to branching morphogenesis and proximal-distal patterning of the embryonic chick lung (Fernandes-Silva et al., 2017).

Considering the morphological and molecular similarities with mammalian lung, the chick developing lung, has emerged as a reliable model to study branching morphogenesis. Furthermore, it presents several additional advantages when compared to mammalian models, for example: it does not

need special housing facilities, its development is progenitor-independent, it is cheaper, it is easy to manipulate surgically and allows a direct observation of embryogenesis.

1.2.4 Retinoic Acid: Modulator of Branching Morphogenesis

Retinoic acid, the active metabolite from Vitamin A, is a crucial growth factor which modulates pivotal cellular processes namely, proliferation, differentiation and apoptosis thus contributing to the morphogenesis of different organs and to the homeostasis of the adult organism (Zachman, 1995; Niederreither et al., 2001; Wilson et al., 2003). This lipophilic molecule has a long-range signaling capacity, it is able to cross biological membranes and form tissue gradients (Fex & Johannesson, 1988). Such characteristics may account for RA widespread bio-functionality in different systems including vision, reproduction, immune system, nervous system, skin health and numerous aspects of the early embryo development (Duester, 2008; Tang & Gudas, 2011).

In the mammalian lung, RA signaling is of major importance during early lung development, primary bud formation, branching morphogenesis and alveologenesis (Zachman, 1995; Malpel et al., 2000; Maden, 2004). During primary lung formation, RA is part of a major regulatory network, RA-TGFβ-*fgf10*, which represents the molecular basis for lung primordium formation (Chen et al., 2007; Chen et al., 2009). RA is also implicated in branching morphogenesis. Indeed, *in vitro* RA supplementation (1 μM), for 96 hours, resulted in an increase in the number of peripheral buds and epithelium perimeter, and expansion of the total area of rat lung explants (Pereira-Terra et al., 2015). Previous studies, in the mouse model, also demonstrated that 1 μM RA treatment, for 48 hours, promotes lung branching (Schuger et al., 1993). More recently, the presence of RA signaling pathway machinery was described in the embryonic chick lung. Interaction studies, using this model, disclosed the role of RA in a complex molecular network during lung branching morphogenesis. In fact, RA increases chick lung branching in a dose-dependent manner and has a role in proximal-distal patterning (Fernandes-Silva et al., 2017). Finally, RA seems to be quite important during alveologenesis, since RA postnatal treatment increases the number of pulmonary alveoli in rats (Massaro & Massaro, 1996). Moreover, RA is associated with alveolar regeneration in adult mouse models of alveoli disruption (Hind & maden, 2004), and prenatal treatment with RA stimulates alveologenesis of CDH hypoplastic lungs (Montedonico et al., 2008).

The following sections will be devoted to exploring the process of Vitamin A transformation into RA, the molecular mechanisms underlying RA signaling cascade namely how RA is able to modulate the transcription of more than 500 genes that display a panoply of functions.

1.3 Vitamin A Metabolism

Vitamin A is a fat-soluble substance that belongs to a group of nutrients that include dietary retinyl esters from animal origin, and provitamin A carotenoids from vegetal source of which β-Carotenes are the most abundant form (Ross et al., 2001). Retinyl esters can be found in a variety of daily consumption products as for instance milk, eggs, fish liver oil and tuna fish; some fruits (mango, melons, apricots) and vegetables (red peppers, carrots, sweet potatoes) are also enriched in carotenoids (Wichterle et al., 2002).

In the adult, the Retinoids metabolic journey begins with the ingestion of a Vitamin A rich diet. Retinyl esters, vitamin A of animal origin, undergo hydrolysis in the stomach. However, it is in the small intestine where the main process occurs, and the major part of retinyl esters are hydrolyzed and converted into Retinol. In fact, this process happens in the intestinal lumen at the brush border membrane, prior to enterocyte absorption. At this level, retinyl esters are converted into Retinol through the activity of a series of Retinyl Esterases (RESs), namely Pancreatic Lipases (LP) (Reboul et al., 2006). Retinol is then able to enter the enterocyte through passive diffusion, depending solely on a Retinol gradient (During & Harrison, 2007). On the other hand, β-Carotenes absorption is mediated by membrane transporters present in the enterocyte membrane, namely the superfamily of Scavenger membrane-bound receptors and particularly the Scavenger Receptor, class B, type 1 (SCARB1) (van Bennekum et al., 2005). Once inside the cells, β-Carotenes are converted into Retinal with the assistance β-carotene-15, 15'-Monooxygenase 1 (BCMO1) that promotes the cleavage of each β-Carotene chain into two molecules of Retinal (Lobo et al., 2013). Retinal from β-Carotenes is then converted into Retinol. Since retinoid molecules are insoluble in water they need to associate with proteins. Thus, to be transported to the Endoplasmic Reticulum, Retinol combines with Cellular Retinol Binding Protein 2 (CRBP2), which is generally highly expressed in the enterocytes (Crow & Ong, 1985). In the endoplasmic reticulum, Retinol is esterified with fatty acyl moieties in order to generate Retinyl esters through the activity of two different enzymes: Diacylglycerol O-acyltransferase 1 (DGAT1) and Lecithin Retinol Acyltransferase (LRAT) (Shih et al., 2009). Afterwards, Retinyl esters and other digestive lipids are combined into chylomicrons, so that they can be transported in the bloodstream and in the lymphatic system to reach the organs, among them the liver (Blomhoff et al., 1982).

The hepatic tissue is the main storage of retinoids in the organism, and has a crucial role as regulator of Vitamin A metabolism. Interestingly, Retinyl esters storage is the result of an evolutionary mechanism developed by vertebrates to survive upon external fluctuation of Vitamin A supply and, in addition to the liver, Retinyl esters can also be stored at high concentrations in the lungs and kidneys (Schmitz et al., 1991).

Since in the liver, Retinyl esters are quickly hydrolyzed into Retinol through the activity of a series of enzymes that are hepatocyte-specific. Then, Retinol is transferred to a subset of hepatic cells named Hepatic Stellate Cells (HSCs), where Retinol will remain as Retinyl Esters, in lipid droplets. This liver storage strongly depends on the dietary Retinoid status (Moriwaki et al., 1988). During this metabolic step, LRAT plays the pivotal function of Retinol esterification into Retinyl esters and also contributes to the formation of the lipid droplets (Batten et al., 2004; Liu & Gudas, 2005; O'Byrne et al., 2005).

When other organs and tissues require Retinoids for their function, the organism consumes the hepatic tissue storage. For that purpose, HSCs Retinyl esters are hydrolyzed into Retinol through RESs (Mentlein & heymann, 1987). Given that the resulting Retinol, in the hepatocytes, is water-insoluble, these molecules must associate with Retinol Binding Proteins (RBP) before entering the bloodstream (Goodman, 1980; Quadro et al., 1999). In fact, the majority of Retinol present in the circulatory system is found as a RBP4 complex (Ong, 1994; Li & Norris, 1996), and the absence of RBPs leads to reduced blood Retinol levels and, consequently, Vitamin A deficiency (Quadro et al., 1999). When this complex reaches the target tissues it interacts with a specific membrane receptor, STRA6 (Stimulated by Retinoic Acid 6) that recognizes RBP and moves Retinol into the cytoplasm (Kawaguchi et al., 2007). In Figure 3, the major events of retinoids metabolism are illustrated.

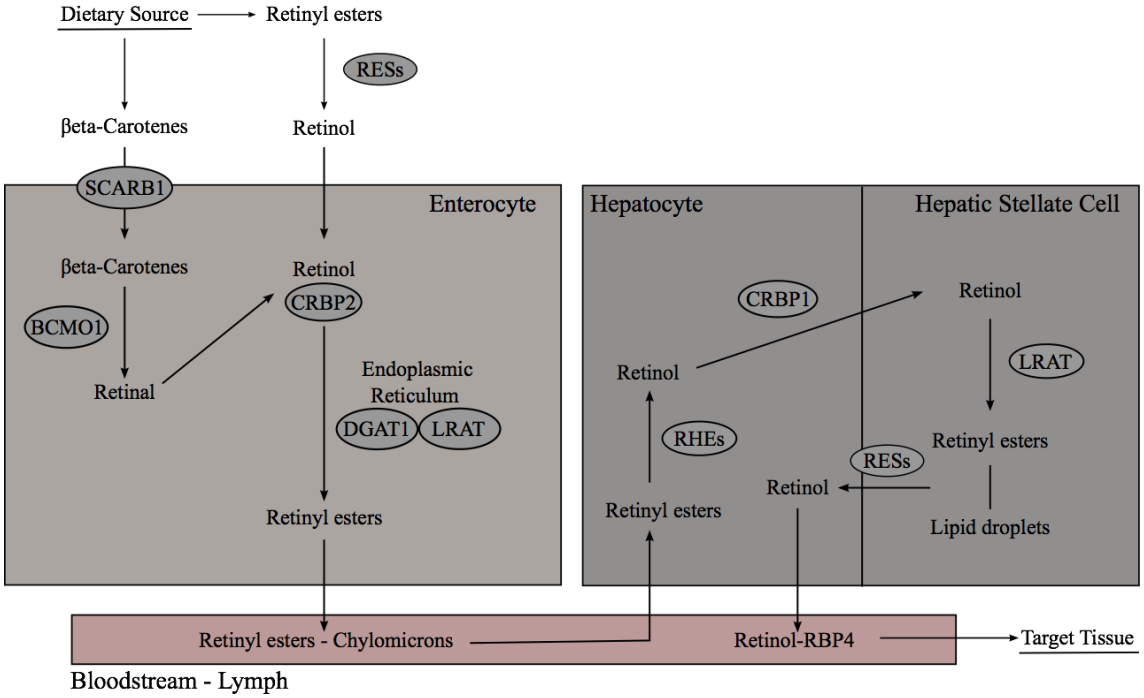

Figure 3 – Retinoids Metabolism. Retinoids metabolism begins with the absorption of Retinyl esters and β-Carotenes from dietary sources. At the enterocyte level, Retinyl esters are hydrolyzed by RESs into Retinol and, on the other hand, β-Carotenes are handled by SCARB1. Afterwards, β-Carotenes are cleaved into Retinal by BCMO1 and then transformed into Retinol. Due to its hydrophobic properties, Retinol from both origins needs to aggregate with CRBP2 to travel inside the cell. Once in the endoplasmic reticulum, Retinol is esterified by DGAT1 and LRAT into Retinyl Esters to travel in the bloodstream in association with chylomicrons up to the liver. In the hepatic tissue, Retinyl esters are converted into Retinol by RHEs and transported by CRBP1 to the Hepatic Stellate Cells (HSCs). Inside HSCs, Retinol is esterified into Retinyl esters by LRAT in order to constitute the Retinoid hepatic storage, in association with lipid droplets. Upon demand, Retinyl esters are converted into Retinol by RESs and can travel via bloodstream combined with RBP4 proteins to reach the target tissue.

1.4 Retinoic Acid Signaling Pathway

When Retinol reaches the target tissue, it may enter the cells through two distinct mechanisms. The first one requires STRA6 membrane transporter, which binds RBP with high affinity and it is able to transport Retinol into the cytoplasm. STRA6 is critical in the heart, diaphragm, eye and the lung. Supporting this data are human *Stra6* mutations, which lead to a series of abnormalities among them pulmonary hypoplasia, CDH, several cardiovascular and eye defects such as anophtalmia and microphtalimia (Pasutto et al., 2007; Golzio et al., 2007; Berry et al., 2013). Nonetheless, some studies suggest that STRA6 is not essential in all biological systems, which points to an alternative route. The second mechanism of Retinol entrance in the cells is by membrane diffusion, as a result of Retinol hydrophobic structure, which depends on the concentration gradient across the cellular membrane and, for this reason, it is not possible to control the amount of Retinol entering the cell (Metzler & Sandell, 2016).

Cytosolic Retinol molecules are water-insoluble and need to associate with CRBP to move through the cytoplasm (Noy & Xu, 1990). Subsequently, Retinol-CRBP1 may have two possible destinations: to be esterified into Retinyl esters by LRAT and to be stored inside the cell, or undergo a series of oxidative steps to generate RA. The oxidative pathway begins with the reversible Retinol oxidation into Retinaldehyde (also named Retinal) by the contribution of several members of Alcohol Dehydrogenase (ADH) and Retinol Dehydrogenase (RDH) enzyme families (Duester, 1998; Kumar et al., 2012). Among them, ADH1, ADH3, ADH4, RDH1, and RDH10 seem to play decisive roles in this enzymatic step (Duester, 2008). In fact, ADH knockout studies disclosed a role for ADH enzymes in retinol clearance to prevent Vitamin A toxicity, and also in generating RA under vitamin A deficiency conditions. In addition, RDH10 point mutations revealed that this enzyme plays a critical role in the generation of considerable amounts of Retinal that serve as substrate for the synthesis of RA during embryonic development (Kumar et al., 2012). Afterwards, Retinal is converted into RA in an irreversible oxidative reaction catalyzed by several Retinaldehyde Dehydrogenases (RALDH) of which there are three main subtypes, RALDH1, RALDH2 and RALDH3. Each RALDH display a tissue-specific expression pattern. Moreover, RA synthesis reaction seems to be carried out predominantly by *raldh2*, at least during early embryonic development; in fact, in *raldh2* (-/-) mutants, embryo development is arrested and RA synthesis is almost completely abolished (Mic et al., 2002).

At this point, the RA that is being produced starts to accumulate inside the cells. To avoid detrimental concentrations, cells developed regulatory mechanisms to control intracellular RA levels. One of the mechanisms depends on Cytochrome P450 (CYP) subfamily 26 enzymes, namely subtypes CYP26A1, CYP26B1 and CYP26C1 that are able to degrade the excess of RA, thus regulating the availability of this molecule for signaling. Among them, CYP26A1 seems to be particularly important during embryonic development in the clearance of the excess of RA (Ross et al., 2001).

RA may act in the producing cell (Autocrine Signaling) or act in a neighboring cell or tissue (Paracrine Signaling). In both cases, RA is transferred into the nucleus of the target cell associated with Cellular Retinoic Acid Binding Protein 2 (CRABP2) and it is able to directly modulate the transcription of target genes. For that, RA binds to specific nuclear receptors, namely Retinoic Acid Receptor (RAR) of which there are three subtypes RARα, RARβ and RARγ (Chambon, 1996). On its turn, RAR binds to Retinoic X Receptor (RXR) and this heterodimer specifically recognizes DNA sequences, named Retinoic Acid Response Elements (RARE), located in the promoter region of RA target genes thus modulating transcription (So & Crowe, 2000). In Figure 4, the main events of RA signaling pathway are illustrated.

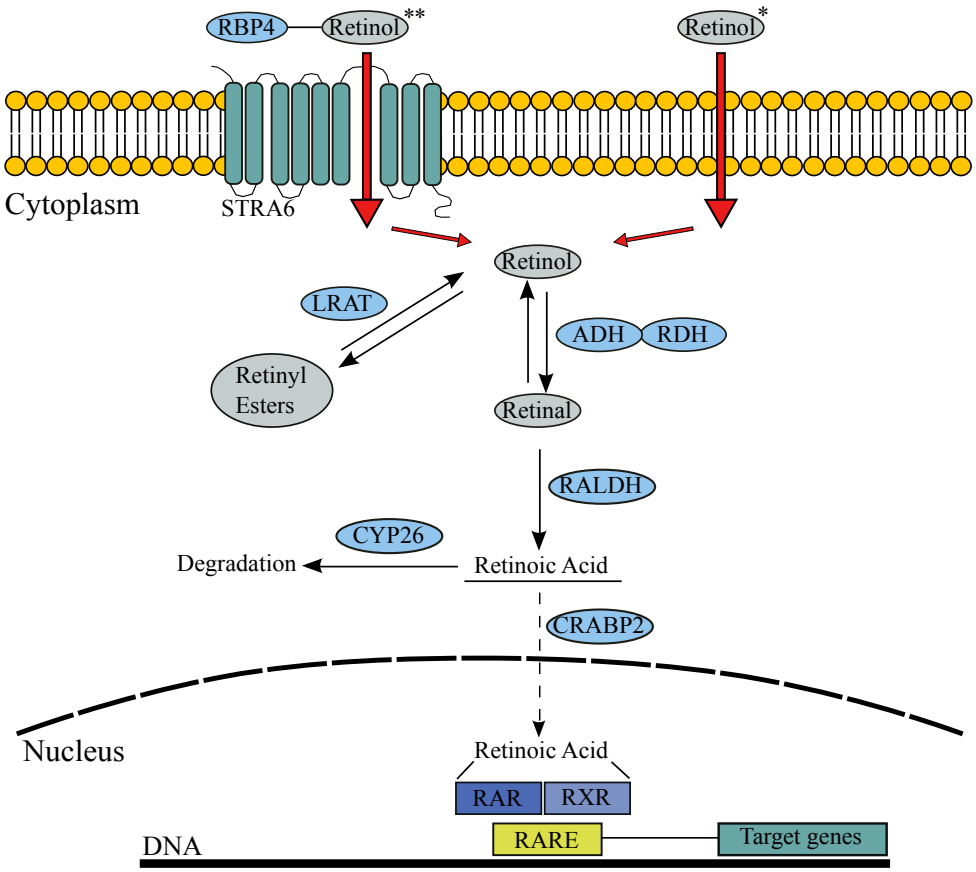

Figure 4 – Retinoic Acid Signaling Pathway. Retinol travels in the bloodstream in association with RBP4. Once in the membrane surface of the target cell, it can enter by diffusion (*) or through the membrane transporter STRA6 (**). Inside the cell, Retinol can be converted into Retinyl esters by LRAT to serve has cellular storage, or be transformed into Retinal by RDH and ADH enzymes. Afterwards, Retinal is oxidized to RA by RALDH. The balance of RA, inside the cell, is meticulously controlled by degradative enzymes such as CYP26. Finally, the available RA is transported into the nucleus bound to CRABP2. In this compartment, it interacts with specific nuclear receptors RAR and RXR which form a heterodimer that recognizes RARE sequences in the promoter region of target genes, thus modulating their transcription.

1.4.1 Retinoic Acid Transcriptional Regulation

RA signaling transduction culminates at the transcriptional level, by modulating the expression of more than 500 genes (Cunningham & Duester, 2015). RA-RAR-RXR complex binds to RARE and induce conformational changes that ultimately promote the replacement of co-repressors by co-activators, namely Nuclear Receptor Co-activators (NCOA). These co-activators are able to recruit Histone Acetylase (HAT) and Trithorax proteins, which promote chromatin relaxation and, consequently, induce the transcription of the target genes (McInerney et al., 1998; Kashyap & Gudas 2010). On the other hand, when RA is absent, RAR-RXR heterodimers bind to RARE in the promoter region of target genes and recruit co-repressors, among them the Nuclear Receptor Co-repressors (NCOR). Then, NCOR recruits repressive factors such as Histone Deacetylase (HDAC) and Polycomb Repressive Complex 2 (PRC2). This results in chromatin condensation and consequently gene silencing (Nagy et al., 1997). Nevertheless, there are

exceptions to this classical mechanism and some genes may be repressed by RA. In this case, in the presence of RA, RAR recruits PRC2 and HDAC and represses gene transcription in a mechanism that is not fully understood (Kumar & Duester, 2014).

1.5 Retinoic Acid and Metabolic Modulation

The biological systems require energy as driving force of all the biochemical reactions and cellular processes. This energy is supplied by nutrients from three main origins: carbohydrates, lipids and proteins. Moreover, these compounds also provide carbons to form new cells and biomass. This complex process is achieved by the coordinated interplay between different metabolic mechanisms modulated by transcription and growth factors. Numerous studies have revealed that RA signaling cascade has a crucial role in numerous cellular processes and as a modulator of metabolic activity. Indeed, RA has been considered crucial and/or with potential therapeutic applications in diverse metabolic disorders, most likely due to the role of RXR-PPARγ heterodimer as a metabolic modulator (Tripathy et al., 2016). In the following sections, some examples of the RA-metabolism relationship, in diverse systems, will be presented.

1.5.1 Retinoic Acid and Glucose Metabolism

Glucose is a six-carbon sugar and it is the most important carbohydrate fuel for animals. Indeed, glucose can have three main fates in the organism: 1) Pentose Phosphate Pathway to produce NADPH and ribose-5-phosphate for nucleotide synthesis; 2) Glycogen production, to be stored in the muscles and liver; 3) Pyruvate production through glycolysis which, then, can have several destinations to produce metabolic intermediates and energy. Glucose can be obtained through alternative mechanisms, namely gluconeogenesis and glycogenolysis, and its physiologic homeostasis is normally maintained by two endocrine hormones, insulin and glucagon.

Over the years, some evidences were disclosed showing a possible relation between RA and glucose metabolism. For instance, hepatic Vitamin A is elevated in diabetic patients; liver glycogen storage is depleted in rats exposed to vitamin A deficient (VAD) diet; and, on the opposite, a Vitamin A rich diet causes an increase in the levels of fasting hepatic glycogen (Moore, 1937; Wolf et al., 1957; Singh et al., 1968). Further reports have shown that RA seems to modulate the expression levels of *gck* (Glucokinase) in rat hepatocytes primary culture, in a synergetic mechanism involving triiodothyronine, RA and insulin (Decaux et al., 1997; Cabrera-Valladares et al., 2001). In fact, Glucokinase is crucial to maintain glucose

homeostasis and its expression levels are lower in rats exposed to VAD diet, which can be reverted upon RA supplementation (Chen et al., 2009). Additionally, RA seems to stimulate the expression of liver *pck1* (Phosphoenolpyruvate Carboxykinase), which is normally suppressed by insulin and induced by glucagon. This gene is responsible for the conversion of oxaloacetate into phosphoenolpyruvate during gluconeogenesis. In fact, reports show that when RAR and RXR heterodimers are activated, the expression of both *pck1* and *gck* is induced (Lucas et al., 1991; Chen et al., 2009).

Yet, specific retinol transporters such as RBP4 proteins are increased in insulin resistant conditions, in both humans and mice with type 2 diabetes. In fact, RBP4 overexpression or injection of recombinant RBP4 in normal mice induced an insulin resistance phenotype. These results point to RBP4 as a potential therapeutic target for treating type 2 diabetes and alter insulin sensitivity (Yang et al., 2005; Graham et al., 2006).

1.5.2 Retinoic Acid and Lipid Metabolism

Lipids are a central nutrient widely used by animals to obtain energy. Indeed, the energy released by lipids (38 kJ/g) doubles the energy obtained from carbohydrates or proteins which makes lipids an excellent energetic storage. Furthermore, lipids are also crucial as components of biological membranes and as signaling molecules. In the organism, lipids are transported in the bloodstream in association with lipoproteins and their metabolism depends on liver activity.

Lately, RA has emerged has a potential modulator of lipids metabolism. In particular, *in vivo* mice studies showed that RA treatment induces a shift in hepatic lipid metabolism, by increasing lipid catabolism and inhibiting lipid biosynthesis. Upon RA supplementation, the expression of hepatic fatty acid oxidation receptors and enzymes is increased, whereas lipogenesis molecular machinery is decreased (Amengual et al., 2010). RA treatment reduced triacylglycerol liver content and circulating VLDL lipoproteins, suggesting a decrease in lipid storage, and caused a reduction of the body weight and fat mass in these animals (Amengual et al., 2010).

RA also has a strong impact on adipocyte metabolism, namely on mitochondrial function. Microarray studies showed that RA upregulates mitochondria related genes. In fact, 62 of a total of 105 genes from oxidative phosphorylation are stimulated by RA, and oxygen consumption increased by 15% (Tourniaire et al., 2015). Additionally, RA seems to have a strong impact on the mitochondrial biogenesis and function. RA modulates transcription factors which are typically associated with the transcription and replication of mitochondrial DNA, thus increasing the number of mitochondria and thermogenic capacity

of white adipose tissue (Mercader et al., 2007; Tourniaire et al., 2015). Regarding mouse skeletal muscle, RA seems to induce an increase in fatty acid oxidation (Amengual et al., 2008).

1.5.3 Retinoic Acid and Protein Metabolism

Regarding protein metabolism, proteolysis seems to be increased in the skeletal muscle of rats exposed to VAD diet. Indeed, vitamin A deficiency elicits an increase of protein catabolism and the induction of urea cycle in these animals (Esteban-Pretel et al., 2010). From the three (carbohydrates, lipids and proteins), RA-protein metabolism interactions seem to be the less explored field.

1.6 Lung Energetic Metabolism

The lung is a metabolically active organ involved in gas-exchange, clearance of the air, secretion of substances, among many other functions. The metabolic profile of the respiratory system was extensively studied during the 70's and 80's (Tierney, 1974; Fisher, 1984). In fact, taking advantage of rat lung perfusion techniques, tissue slices and glucose labeled with tritium or radioactive carbon isotypes, it was possible to measure lung glucose consumption rate and carbon flow. From this data, it was suggested that the adult lung metabolic requirements, at least in part, are achieved through glucose catabolism, even though adult lung tissue glucose reserves are minimal (von Wichert, 1972; Basset & Fisher, 1976a). The major paths from glucose metabolism supply products such as glycerol-3-phosphate, lactate, pyruvate, CO_2 and ribose that are critical for nucleic acid, lipids and amino acid synthesis. Glucose catabolism also generates NADPH (from pentose shunt) and NADH (from glycolysis), plus high energy compounds such as ATP.

In order to understand how glucose carbons were metabolized, perfused lungs were exposed to glucose labeled with ^{14}C (Basset & Fisher, 1976b). With this approach, it was possible to determine that approximately 50% of glucose carbons were metabolized into lactate and pyruvate. From this fraction, the production of lactate was 10-fold greater than pyruvate and it was considered high in comparison with other organs such as the heart (Basset & Fisher, 1976b). CO_2 is also a major product from glucose oxidation. In fact, it is considered that ¼ of CO_2 is produced by pentose shunt, ¼ from pyruvate dehydrogenase reaction and ½ from Tricarboxylic Acid Cycle (TCA) (Basset & Fisher, 1976a). Additionally, a lower percentage of carbons from glucose are used for polysaccharides biosynthesis (Basset & Fisher, 1976b). Glucose carbons are also utilized for protein synthesis contributing to alanine production, through pyruvate transamination (Yeager & Massaro, 1972). Furthermore, carbons from glucose also contribute

for lipid biosynthesis, however the precise distribution of these carbons may depend on the availability of fatty acids in the perfusion medium, animal nutritional status and the animal age (Basett et al., 1981).

Pulmonary tissue is known to have a pronounced capacity in esterifying free fatty acids and incorporation of acetate into lipids. Moreover, the adult lung is able to oxidize fatty acids from plasma lipoproteins and from free nonesterified fatty acids (Felts, 1964). Indeed, the adult lung lipid storage is more than sufficient to feed mitochondria for many hours, via acetyl-CoA, suggesting a role for lipid oxidation as an energetic source (Tierney, 1974). Adult pulmonary metabolism is also recognized to have a high lipid biosynthesis rate, to carry out lung surfactant production. Pulmonary surfactant is responsible for reducing the surface tension at the air-liquid interface and increasing the elasticity compliance in the terminal airways, thus avoiding alveolar collapse. In the mammalian lung, surfactant is composed by 90% of lipids and 10% of proteins (Veldhuizen et al., 1998), and it is produced and secreted by type II alveolar cells (Klaus et al., 1962). Curiously, other species which do not exhibit alveoli, such as birds, also depend on surfactant fluid; in this case, it is believed that surfactant is important to maintain air-flow and might have additional functions (Bernhard et al., 2001). However, nothing is known regarding the metabolic profile of the lung during development.

1.7 Retinoic Acid, Metabolism and Lung Branching Morphogenesis

Lung development is a complex process governed by epithelium-mesenchyme interactions and regulated by several transcription and growth factors (Ornitz & Yin, 2012). At early stages of development, mammalian and chick lung are quite similar in terms of structure, and the molecular mechanisms underlying branching morphogenesis seem to be conserved (Moura et al., 2011; Moura et al., 2014; Moura et al., 2015; Fernandes-Silva et al., 2017). Branching morphogenesis depends on activation of conserved signaling pathways, among them RA. In fact, RA signaling is essential during vertebrate embryonic development in processes such as proliferation, differentiation, and morphogenesis of several organs, including the lung (Duester, 2008). Furthermore, lung branching is expected to have a high-energy consumption rate since, in this stage, lung tissue undergoes numerous cellular processes that are known to require elevated amounts of energy and carbons for biomass. In fact, glucose uptake and metabolism are essential for the survival and proliferation of cells and are supposed to be enhanced in embryonic systems like the developing lung (Ito et al., 1999). Some of the glucose catbolism pivotal elements, as for instance glucose transporters are known to be sensitive to cytokines, hormones, and growth factors (Wagstaff et al., 1995; Humphrey et al., 2004). Moreover, glucose catabolism is proposed

to serve as energy supply but also as a way to facilitate the uptake of nutrients to form biomass and new cells. This is true not only in cancer but also in developing systems, and is also controlled by growth factors that regulate the activity and expression of specific enzymes (Ito et al., 1999; Oliveira et al., 2015).

RA is one of the growth factors that is likely to modulate the metabolic process in the avian lung, due to its positive effect in early stages of chick lung branching (Fernandes-Silva et al., 2017). Moreover, several studies suggested RA as a modulator of metabolism in organs such as the liver, adipocytes, skeletal muscle and in several metabolic disorders, namely diabetes. In fact, RA seems to have the capacity to modulate the glucose catabolism machinery, mitochondrial biogenesis, mitochondrial function, oxidative phosphorylation, lipid biosynthesis, lipid catabolism, protein catabolism and many other metabolic aspects (Lucas et al., 1991; Amengual et al., 2010; Esteban-Pretel et al., 2010; Tourniaire et al., 2015).

Nevertheless, the relationship between RA and metabolism, in the developing lung is still unknown. The disclosure and characterization of this association, during embryonic lung development, more precisely during branching morphogenesis is of great importance to reveal novel therapeutic approaches that may contribute to treating lung disorders.

2. AIMS

Retinoic acid is a crucial growth factor for embryonic development and, particularly, to lung morphogenesis. This potent morphogen strongly influences chick lung branching and may be a metabolic modulator of the developing lung. In this work, we aim to characterize, for the first time, the metabolic profile of chick lung branching and to uncover the potential interaction between RA and lung metabolism. For this purpose, we intend to describe the metabolite fluctuations associated with normal and RA-induced metabolism, during *in vitro* chick lung development, by ^{1}H-NMR spectroscopy. Furthermore, the expression pattern and levels of key metabolic genes will be assessed by *in situ* hybridization and qRT-PCR, respectively. With this approach, we intend to bring new insights about specific metabolic biomarkers that might unravel new therapeutic strategies for lung disorders treatment. Moreover, we aim to clarify the impact of RA on metabolic pathways associated with embryonic lung development.

This thesis aims to accomplish the following specific objectives:

1 – Characterize the expression pattern of metabolic enzymes and transporters, by *in situ* hybridization.

2 – Characterize metabolite fluctuations during normal chick lung branching, by ^{1}H-NMR spectroscopy and using an *in vitro* lung explant system.

3 – Characterize RA-induced metabolite fluctuations during chick lung branching, by ^{1}H-NMR spectroscopy and using an *in vitro* lung explant culture.

4 – Assess the expression levels of key metabolic enzymes and transporters in normal and RA-induced metabolism, by qRT-PCR.

5 – Disclose interactions between RA and lung metabolic processes.

3. Materials and Methods

3.1 Ethical Issues

According to the Directive 2010/63/EU of the European Parliament and the Council of 22 September 2010 on the protection of animals used for scientific purposes, and the Portuguese Directive 113/2013 of 7 August 2013, this work, performed at early stages of chicken development, does not need ethical approval from review board institution or ethical commissions.

3.2 Eggs and Tissue Collection

Fertilized chicken eggs, *Gallus gallus*, were incubated between 4.5 and 5.5 days in an incubator with 49% humidified atmosphere and 37°C of temperature (Termaks KB400, Norway). HH24-26 stage embryos (Hamburger & Hamilton, 1951) were dissected in PBS (0.8% NaCl, 0.02% KCl, 0.02% KH_2PO_4, 0.12% $Na_2HPO_4.2H_2O$) using surgical microdissection material (FST, Germany) under a stereomicroscope (Olympus SZX16, Japan), to obtain whole lungs. Subsequently, lungs were classified in stage b1, b2 or b3 according to the number of secondary buds emerging from the main bronchus (Moura et al., 2011). Dissected lungs and whole embryos were processed for *in situ* hybridization and were fixated in a formaldehyde solution (4% formaldehyde in PBS, 2 mM EGTA, pH 7.5) at 4°C, overnight. Subsequently, lungs were dehydrated through a PBT (PBS with 0.1% of Tween 20)/methanol series and stored at −20 °C. Lungs were also collected in PBS for *in vitro* lung explant culture. Moreover, HH24 embryos were collected and snap frozen for total RNA extraction.

3.3 Whole Mount *in situ* Hybridization

In situ hybridization is a semi-quantitative technique that allows the detection of a specific mRNA in tissues through the hybridization of an antisense RNA probe complementary to the target gene. The antisense probe is synthesized by an *in vitro* transcription reaction and labeled with digoxigenin. Digoxigenin is recognized by a specific antibody coupled to an enzyme, alkaline phosphatase, responsible for catalyzing a colorimetric reaction allowing the identification of the mRNA-antisense probe hybrid. With this technique, it is possible to assess and characterize gene expression localization, and to compare relative levels of expression in samples processed simultaneously. Since the probes used in this work were not available in the literature, it was necessary to clone part of the coding region of the genes of interest into a specific plasmid, to use as a template to produce the mRNA probe.

3.3.1 Antisense mRNA Probe Synthesis

Total RNA from HH24 embryos was obtained using TripleXtractor directRNA kit (Grisp, Portugal), following the manufacturer's instructions, and stored at -80°C. RNA concentration and absorbance ratios (A260/A280) were determined using Nanodrop (NanoDrop ND-1000, USA). Subsequently, total RNA was treated with DNase I (Thermo Scientific, USA), to eliminate possible DNA contamination. Through a reverse transcription reaction, cDNA was produced from treated RNA (maximum μg possible), using GRS cDNA Synthesis kit (Grisp), and stored at -20°C. cDNA concentration was determined by Nanodrop (ND-1000).

cDNA was used as template to amplify part of the coding region of the genes of interest, by conventional PCR (GRS Xpert Taq 2x MasterMix, Grisp). Specific primers were designed based on predicted sequences annotated in the chicken genome (Table 1). The presence of the fragments was assessed by agarose gel electrophoresis. Resulting PCR fragments, with the expected size, were cloned in a commercial plasmid pCR™II TOPO® (Thermo Scientific). This vector was selected because it contains specific sites for universal primers (M13 forward and reverse), ampicillin resistance, the lacZ promoter, the promoter region of Sp6 and T7 RNA polymerases, and single overhanging 3´ deoxythymidine (T) residues. Since Taq polymerase adds a single deoxyadenosine (A) to the 3´ ends of PCR products it facilitates its insertion in this vector. TOPO® TA Cloning® Kit was used according to the manufacturer´s instructions. *Escherichia coli* (XL1-blue) competent cells were transformed with the TOPO cloning reaction, by heat shock protocol, according to (Green & Sambrook, 2012). Cells were plated on LB (0.5% yeast extract, 1% NaCl, 1% tryptone, 2% agar) culture medium, supplemented with ampicillin 1 μg/mL, X-gal and IPTG (for blue-white screening) and then incubated overnight at 37°C. White colonies were inoculated in LB liquid supplemented with ampicillin 1 μg/mL, and grown at 37°C, 220 rpm, overnight. Plasmid DNA was extracted following (Green & Sambrook, 2012) protocol, and the presence of the insert confirmed by PCR using M13 universal primers. Colonies containing the fragment of interest were re-inoculated in liquid medium, and grown at 37°C, 220 rpm, overnight. In the next day, glycerol stocks were made and for plasmid DNA extraction, GeneJET Plasmid Miniprep Kit was used (Thermo Scientific). Plasmid concentration was determined using Nanodrop (ND-1000) and plasmid integrity was assessed by agarose gel electrophoresis. Subsequently, plasmids were sequenced by light-speed Sanger sequencing method (GATC Biotech, Germany) to confirm that the fragment corresponded to the coding region of the genes of interest and to determine insert orientation.

Before *in vitro* transcription reaction, fragments with the region of interest were obtained by conventional PCR, KAPA2G Fast ReadyMix PCR kit (KapaBiosystems, USA), using M13 universal primers.

For probe synthesis, 1 μg of amplified DNA fragments was used, and the *in vitro* transcription reaction performed according to Dig RNA labeling mix manufacturer (Roche, Germany). Specific RNA polymerase (SP6 for all the genes) was incubated with a nucleotide mixture, in which uracil is labeled with digoxigenin.

Table 1 – Primers sequences for mRNA antisense probe synthesis. Primers sequences forward (FW) and reverse (RV) for PCR fragment amplification, respective product size and annealing temperature.

Genes	Primer Sequence	Product Size	Annealing T(°C)
glut3	FW - ATGTGGCCCCTATGTCTTCC RV - GGCAACTTCTTTGTCAGGTTCT	215	51.9
hk1	Fw - ATCGATAAATACCTTTACGCCATGC RV - TGTCTTTGATTTGTTGTTTCTCCAT	373	48.9
ldha	Fw - GCACTTTCCAAGTAGGTCAAATCC RV - AGTCTTTGGTTTCACGTTGTGT	292	50.7
ldhb	Fw - GCAGGTTGTTGAAAGTGCCT Rv - AGTGAGTAGAGAGCCCACAT	374	51.0
pdha	Fw - CAAGAAGTGAGAAGCAAAAGTGA Rv - TACCTAGCTCTTCCAGTGGGG	175	49.4
pdhb	Fw - TGCGTGTTACAGGTGCAGAT Rv - TGCATACAAGTTGTCCTACACCA	177	52.1

3.3.2 Whole Mount *in situ* Hybridization

In situ hybridization was performed according to (Henrique et al., 1995), with minor modifications. To characterize the expression pattern, n≥9 lungs/stage/gene were used. Firstly, tissues were rehydrated through a methanol and PBT series. Afterwards, tissues were incubated with a proteinase K solution (PBT with 0.05% proteinase K) (Roche). This serine protease acts on membrane proteins thus degrading cell membrane and increasing cell permeability, therefore allowing the probe to enter the cell and binding to the mRNA. The process was thoroughly controlled, according to the size of the tissues: 40 minutes incubation for HH25 embryos and 2 minutes for whole lungs. Additional PBT washes were made to remove excess of proteinase K and, subsequently, tissues were incubated with a post-fixing solution (PBT with 10% formaldehyde, 0.4% glutaraldehyde) to increase the consistency and the mechanic properties of the weakened tissues. After this step, tissues were incubated with hybridization solution (50% formamide, 6.5% SSC, 1% EDTA 0.5 M pH 9.8, 0.25% t-RNA, 0.2% Tween 20, 0.2% heparin, 0.5% CHAPS), at 70°C to enhance the capacity of hybridization, by eliminating RNA secondary structures.

Tissues were incubated with the specific probes, in hybridization solution, at 70°C, overnight. The following day, several washes were performed with preheated hybridization solution, hybridization solution with MABT (50:50) (5.8% $C_4H_4O_4$, 4.4% NaCl, 7% NaOH, 1% Tween 20, pH 7.5) and subsequently with only MABT to remove possible unbound or non-specifically bound probe. Next, tissues were treated with blocking solutions [MABT with 20% blocking reagent (Roche); MABT with 20% blocking reagent plus 20% goat serum (Invitrogen)], to prevent nonspecific antibody binding. Then, lungs were incubated in MABT, 20% blocking reagent, 20% goat serum and 1:2000 anti-digoxigenin antibody (Roche) solution, overnight, at room temperature, with agitation. On day 3, the tissues were washed extensively with MABT solution to eliminate background from unspecific antibody labeling. In the last day, tissues were washed in NTMT solution (0.1 M NaCl, 0.1 M Tris-HCl, 50 mM MgCl2, 1% Tween 20) and then incubated in a developing solution (NTMT with BCIP, NBT) (Roche), at 37°C and protected from light. The developing colorimetric reaction was carefully supervised until the expression level obtained was appropriated and background levels were not reached. The reaction was stopped, at the same time, for the same group of tissues, by washing 3 times in PBT. All the lungs were photographed with a camera (Olympus U-LH100HG) coupled to a stereomicroscope (Olympus SZX16). Lastly, lungs were stored in PBT solution with 0.1% Azide.

3.4 Histological Sections

Selected hybridized chicken lungs were dehydrated through increasing ethanol series and embedded in a 2-hydroxyethyl methacrylate solution (Heraeus Kulzer, Germany). Then, 25 μm thick histological slides were produced by a rotatory microtome (Leica RM 2155, Germany). Lung histological sections were photographed using a camera (Olympus DP70) coupled to a microscope (Olympus BX61).

3.5 *In vitro* Lung Explant Culture

After dissection, lungs were transferred to an *in vitro* lung explant culture system based on an air-liquid interface, composed by 8 μm nucleopore polycarbonate membranes (Whatman, USA) and a nutritive medium. Membranes were presoaked in Medium 199 (Sigma, USA) before the lungs were placed on them. The following procedure was made using a complex medium containing Medium 199 supplemented with 10% (V/V) chick serum (Invitrogen), 5% (V/V) heat-inactivated fetal calf serum (Invitrogen), 1% (V/V) L-glutamine (Invitrogen), 1% (V/V) penicillin 5000 IU/mL plus streptomycin 5000 IU/mL (Invitrogen) and 0.25 mg/mL of ascorbic acid (Sigma). Two different set of experiments were performed (n=6/stage/condition):

1) b1, b2 and b3 lungs were incubated with complex medium;
2) b2 lungs were randomly assigned one of the following experimental groups:
    a. complex medium supplemented with 1 μM of retinoic acid (R2625; Sigma), dose selected according to literature (Cardoso et al., 1995; Fernandes-Silva et al., 2017);
    b. complex medium supplemented with DMSO (1 μL/mL) as control, since it is retinoic acid solvent.

In both cases, chick lungs were kept in culture for 48 hours in 24 well culture plates, at 37°C with a 5% CO_2 atmosphere (Heraeus HeraCell CO_2 incubator, Netherlands) (Moura et al., 2014). Lungs were photographed in the beginning of the culture, at 0 hours (D0). After 24 hours in culture (D1), explants were photographed and the medium replaced with fresh supplemented complex medium, according to the correspondent condition. Finally, after 48 hours in culture (D2), lung explants were photographed again.

D0 and D2 lung explants were collected and stored at -80°C, for RNA extraction. The culture medium was collected at D0, D1 and D2 and stored at -20°C, for ^{1}H-NMR spectroscopy analysis.

3.6 Morphometric Analysis and Branching Measurement

Lung branching was monitored by photographing explants at D0, D1 and D2. For the morphometric analysis, the internal perimeter of the lung (epithelium) was assessed at D0 and D2 using AxionVision Rel. 4.3 software (Carl Zeiss GmbH, Germany), as shown in figure 5. The results of the morphometric analysis were expressed as D2/D0 ratio of the epithelial perimeter, which is a suitable measurement of branching and lung growth.

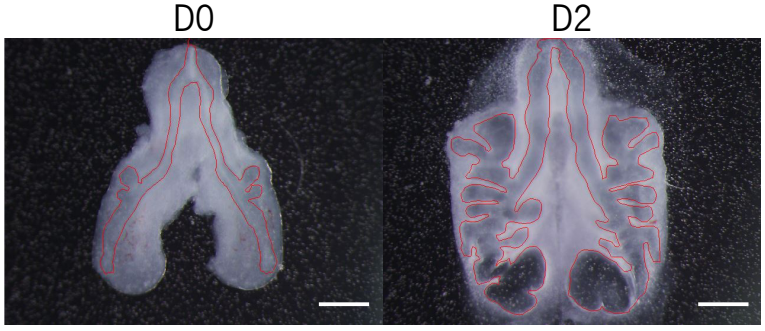

Figure 5 – Lung Explant Perimeters. Representative lung explants at D0 (0h) and D2 (48h), with representation of the epithelium perimeter outlined using AxionVision Rel. 4.3 Software. Scale bar: 500 μm.

3.7 Quantitative RT-PCR

Total RNA was extracted from D0 and D2 lung explants, from the three culture conditions, using TripleXtractor direct RNA kit (Grisp) and stored at -80°C. RNA was processed as previously described to obtain cDNA. Specific exon-exon spanning primers were designed for the amplification of target and housekeeping transcripts; primers were optimized in terms of PCR reaction, namely for annealing temperature and cycles (Table 2). Then, primers were optimized in terms of cDNA dilutions, to ensure they were in the same efficiency range. qRT-PCR was performed using 1 μL of cDNA sample and NZY qPCR Green Master Mix (2x) (NZYTech, Portugal), according to manufacturer's instructions. mRNA expression levels were normalized for *18s* and *actin-β* housekeeping genes, as internal controls. Each sample was ran in duplicate (n=6/condition/stage). Fold variation of gene expression levels was calculated following the mathematical model 2^(-ΔΔCt) (Pfaffl, 2001).

Table 2 – Primers sequences for qRT-PCR. Primers sequences forward (FW) and reverse (RV) for qRT-PCR amplification, respective product size, annealing temperature and PCR cycles.

Genes	Primer Sequence	Product Size	AnnealingT (°C)	Cycles
actin-β	FW - CTTCTAAACCGGACTGTTACCA RV - AAACAAATAAAGCCATGCCAATCT	100	58	30
18s	Fw - TCTTTCTCGATTCCGTGGGT RV - AACGCCACTTGTCCCTCTAC	157	58	30
glut3	Fw - GTACCGTTCGGGTTCCGTTAG RV - AATGGCAGCAACAGAAACAGC	115	62	35
hk1	Fw – CTGGCCTACTACTTCACCGAG Rv - TCACTGTCGCTGTTGGGTTA	166	58	35
ldha	Fw - AAGACGCCGGCAGTACAC RV - GAGTGTGCAGTCACGCTGTA	285	58	35
ldhb	Fw - ACTTGGTATCCACCCAACCAG Rv - CTCAGCAACGCTAAGACCAAT	244	54	35
pdha	Fw - TCACGGCTTTACCTATGCCC Rv - ACCTGAGCACCGACAATACC	153	58	35
pdhb	Fw - GCTCAGAAGATGCTAAAGGGC Rv - GCTTCTAAACAGTGCCCAACAG	220	58	35

3.8 ^{1}H-NMR Spectroscopy

Samples of 200 μL of medium were collected from *in vitro* lung explant culture and submitted to ^{1}H-NMR spectroscopy analysis (n=6/condition/stage). A Bruker Avance 600 MHz spectrometer with a 5 mm QXI probe and z-gradient (Bruker Biospin, Germany) was used and spectra accessed at 25°C (Alves et al., 2013). Solvent-suppressed ^{1}H-NMR spectra were acquired with the following settings: 6 kHz spectral width, 14-second interpulse, 3-second water presaturation, 45-degree pulse angle, 3.5-second acquisition time and minimum of 128 scans (Alves et al., 2012). In order to quantify the extracellular metabolites in the media, sodium fumarate (singlet, at 6.50 ppm, δ parts per million), was used as internal reference, at 1 mM final concentration. The following metabolites were quantified: H1-α glucose (doublet, 5.22 ppm), lactate (doublet, 1.33 ppm), alanine (doublet, 1.46 ppm), pyruvate (singlet, 2.34 ppm), acetate (singlet, 1.9 ppm), glutamine (doublet, 3.7ppm) and glutamate (multiplet, 2.04 ppm). The relative areas of ^{1}H-NMR resonances were quantified using the curve-fitting routine supplied with the NUTSproTM NMR spectral analysis program (Acorn NMR, USA).

3.9 Statistical Analysis

Statistical analysis was performed using GraphPad Prism 6 (GraphPad software, USA). Since all data followed a normal distribution, the statistical significance of the groups was assessed by student t-test or by one-way ANOVA, followed by multiple comparisons through Fisher Least Significant Difference (LSD) method. All experimental data is presented as mean ± SEM with $p<0.05$ considered significant.

4. Results

4.1 Characterization of the metabolic profile of early chick lung branching

The lung is a metabolically active organ and it is responsible for gas-exchange. The metabolic profile of the adult lung has been explored in the past, and results showed it has a strong dependence on glucose catabolism though it is also associated with lipid catabolism and biosynthesis. Nevertheless, the metabolic profile of the developing lung remains unknown. During pulmonary development, several signaling pathways are active and interacting with each other, among them Retinoic Acid signaling. Furthermore, the numerous cellular events that occur during development require high quantities of energy and carbon sources to form new cells. Since glucose seems to actively contribute to the adult lung metabolism, we aimed to characterize glucose catabolism during early lung development using the chicken as a model.

For this purpose, several elements from glucose catabolism machinery were analyzed, among them: *glut3* (glucose transporter 3) that codes for a glucose transporter (GLUT) that is responsible for importing glucose across the membrane into the cell; *hk1* (hexokinase 1) responsible for the first step of glycolysis, the conversion of glucose into glucose-6-phosphate; *ldha* and *ldhb* (lactate dehydrogenase) that code for lactate dehydrogenase enzyme, which is responsible for the interconversion of pyruvate into lactate; *pdha* and *pdhb* (pyruvate dehydrogenase), that are part of the pyruvate dehydrogenase enzymatic complex and essential for the pyruvate conversion into acetyl-CoA. The expression pattern of these enzymes and transporters was assessed, in b1, b2 and b3 stage lungs, by *in situ* hybridization, in order to characterize their spatial localization in the lung tissue. Moreover, lungs from the three stages were processed to *in vitro* lung explant culture and tissues collected for determining the expression levels of the same enzymes and transporters, by qRT-PCR. From the *in vitro* lung explant system, culture medium was collected and extracellular metabolites analyzed and quantified, by ^{1}H-NMR spectroscopy, namely: glucose, in order to determine its consumption; and the three metabolites that derive from pyruvate metabolism such as alanine, lactate and acetate that may arise from acetyl-CoA. With this approach, the metabolite profile of early chick lung branching was characterized.

4.1.1 Characterization of the expression pattern of key metabolic enzymes and transporters

To study the expression pattern of *glut3*, *hk1*, *ldha*, *ldhb*, *pdha* and *pdhb*, b1, b2 and b3 embryonic chick lungs were analyzed by *in situ* hybridization. *In situ* hybridization relies on the use of antisense mRNA probes. Since the probes for the selected genes were not described in the literature, it was necessary to clone the genes in a specific plasmid to facilitate the synthesis of the antisense probes

that will then hybridize with the corresponding mRNA in the tissue, revealing the localization of the transcript. To achieve this, primers were designed for *glut3*, *hk1*, *ldha*, *ldhb*, *pdha* and *pdhb* and amplified by conventional PCR reaction, using cDNA from HH24 embryos and b2 lungs (table 1, section 3.3.1). Subsequently, electrophoresis was performed using a 0.8 % agarose gel to identify the presence of each gene in the embryonic chick lung (Figure 6). All the fragments corresponding to the genes under study were present, both in the whole embryo and in the chick lung.

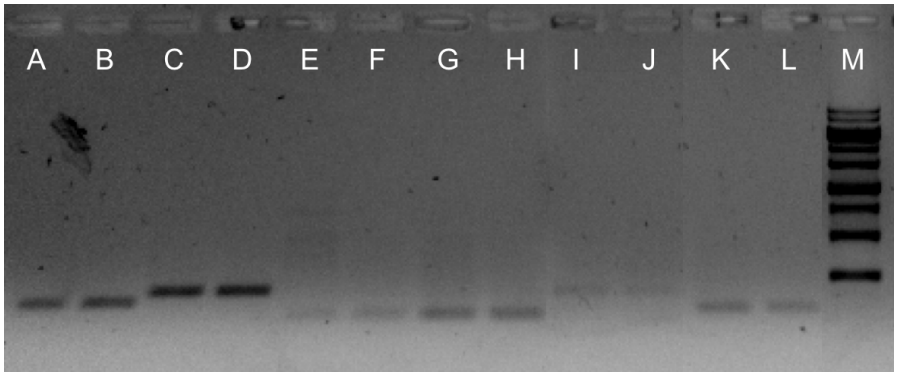

Figure 6 – Detection of amplified fragments by agarose gel electrophoresis. The fragments correspond to: *ldha* (A-B), *ldhb* (C-D), *pdha* (E-F), *pdhb* (G-H), *hk1* (I-J), *glut3* (K-L) and molecular weight size ladder (M). For each gene, the first band corresponds to a HH24 embryo and the second to a stage b2 lung, respectively.

After cloning and sequencing the fragments, antisense probes were synthetized and embryonic lungs processed for *in situ* hybridization. Then, representative lungs of each stage were processed for histological sectioning.

glut3 is expressed in the proximal region of the lung, namely in the tracheal mesenchyme (Fig. 7b, dark arrowhead). *glut3* is absent from the main bronchus epithelium (Fig. 7b, black arrow), but present in the secondary bronchi (Fig. 7c, asterisk). This expression pattern is stage-dependent since it is not detected in b1 stage (Fig. 7a), but highly expressed in b2 and b3 (Fig. 7b and 7c, respectively). Additionally, from stage b2 to b3, the mesenchymal expression expands distally. Histological sectioning confirmed the presence of *glut3* transcript in the secondary bronchi (Fig. 7d, asterisk) and in the surrounding mesenchyme.

hk1 mRNA is present in the tracheal (Fig. 7e, dark arrowhead) and the dorsal mesenchyme (Fig. 7g, dashed arrow). *hk1* is absent from the main bronchus epithelium (Fig. 7f, black arrow). This spatial distribution is consistent in the three stages studied. Hybridized lung sections showed the presence of *hk1* in the dorsal mesenchyme (Fig. 7h) and surrounding the secondary bronchi (Fig. 7h, asterisk).

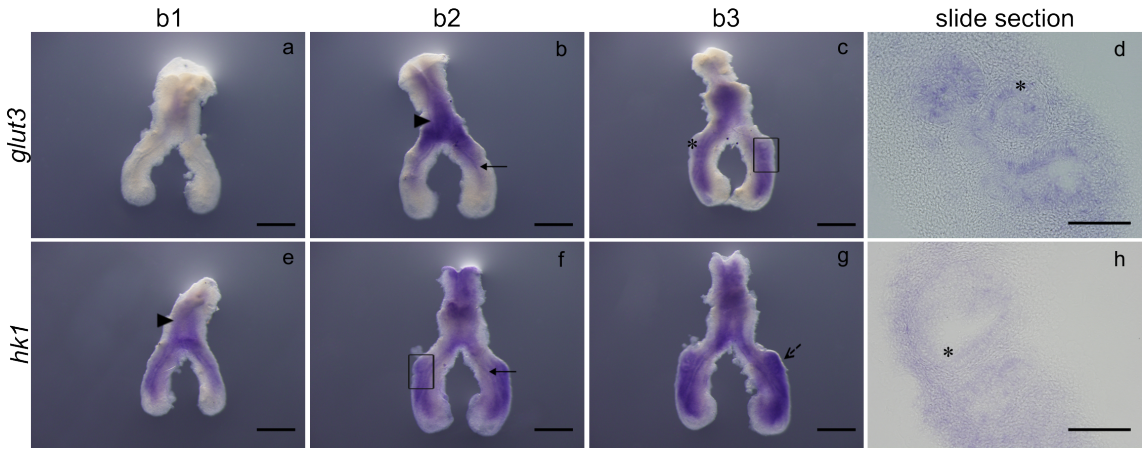

Figure 7 – *glut3* and *hk1* expression pattern at early stages of chick lung development. Representative examples of *in situ* hybridization of stage b1, b2 and b3 lungs for: *glut3* (a-d) and *hk1* (e-h), n≥9 per stage. Scale bar: whole mount, 500 μm; slide sections, 100 μm. The black rectangle in image c and f indicate the region shown in corresponding slide section. Asterisk: secondary bronchi. Black arrow: main bronchus epithelium. Dark arrowhead: trachea region. Dashed arrow: dorsal mesenchyme.

ldha expression is evident in the proximal epithelium of the lung, namely in the trachea region (Fig. 8a, dark arrowhead). *ldha* is also present in the more distal region of the main bronchus (Fig. 8a, dagger) but is lacking from the main bronchus epithelium and secondary bronchi (Fig. 8c, dark arrow and asterisk, respectively). This expression pattern is similar in the three stages studied, but decreases in stage b3. Slide sectioning of hybridized lungs confirmed the presence of *ldha* in both mesenchyme and epithelium of the trachea (Fig. 8d).

ldhb transcript is completely absent from the proximal region of the lung (Fig. 8e, dark arrowhead), and from the primary bronchus epithelium (Fig. 8f, dark arrow). *ldhb* is strongly expressed in the distal most region of the lung (Fig. 8e, dagger) and in the secondary bronchi (Fig. 8g, asterisk). Lung sectioning clearly showed that this gene is not expressed in the distal epithelium but exclusively in the distal mesenchyme (Fig. 8h, dagger).

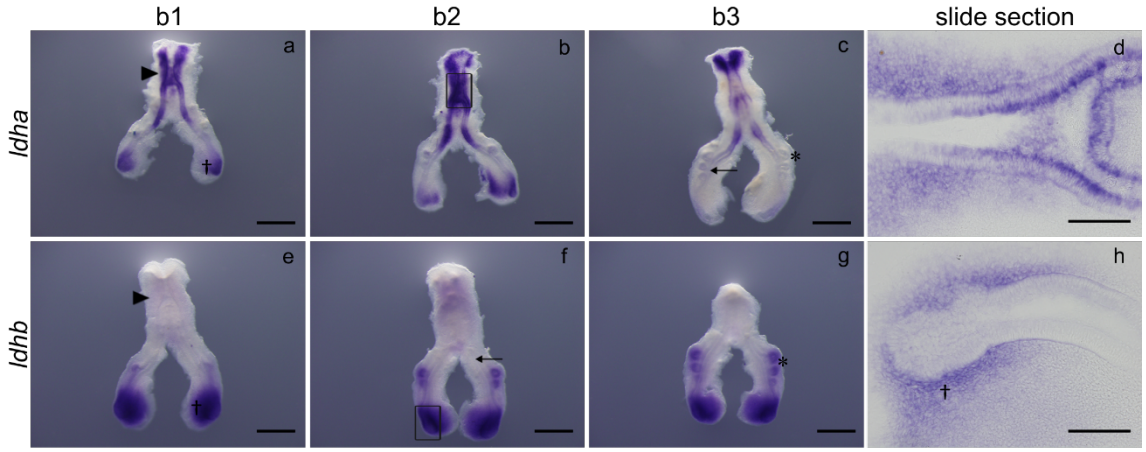

Figure 8 – *ldha* and *ldhb* expression pattern at early stages of chick lung development. Representative examples of *in situ* hybridization of stage b1, b2 and b3 lungs for: *ldha* (a-d) and *ldhb* (e-h), n≥9 per stage. Scale bar: whole mount, 500 μm; slide sections, 100 μm. The black rectangle in image b and f indicate the region shown in corresponding slide section. Asterisk: secondary bronchi. Black arrow: main bronchus epithelium. Dagger: distal mesenchyme. Dark arrowhead: trachea region.

pdha is expressed in the mesenchyme of the trachea (Fig. 9b, dark arrowhead) and strongly expressed in the secondary bronchi (Fig. 9c, asterisk). Sectioning of selected hybridized lungs confirmed that *pdha* mRNA is present in the secondary bronchi (Fig. 9d, asterisk) but absent from the main bronchus epithelium (Fig. 9d, dark arrow).

pdhb expression was not detected in the lungs of the three stages studied (Fig. 9e-g). Due to this fact, histological sections were not performed.

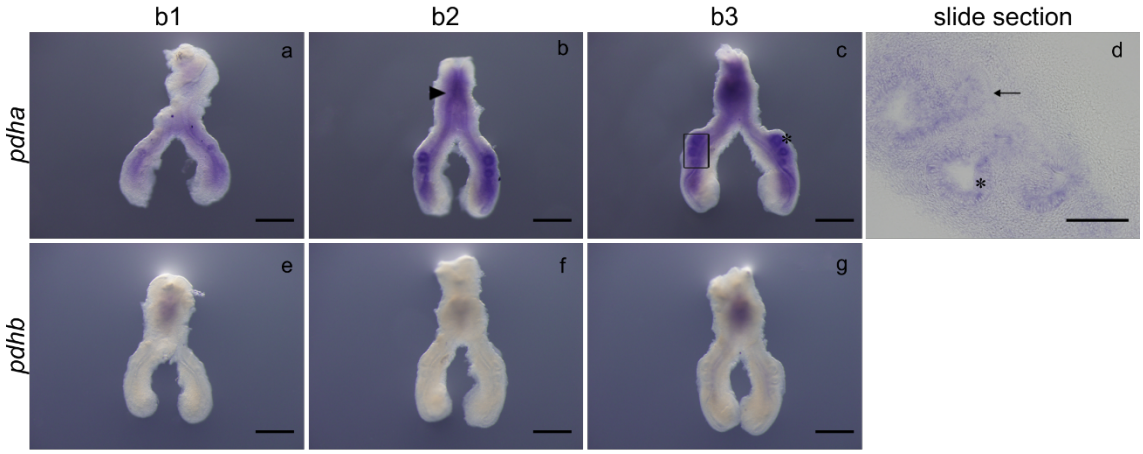

Figure 9 – *pdha* and *pdhb* expression pattern at early stages of chick lung development. Representative examples of *in situ* hybridization of stage b1, b2 and b3 lungs for: *pdha* (a-d) and *pdhb* (e-g), n≥9 per stage. Scale bar: whole mount, 500 μm; slide sections, 100 μm. The black rectangle in image c indicates the region shown in corresponding slide section. Asterisk: secondary bronchi. Black arrow: main bronchus epithelium. Dark arrowhead: trachea region.

4.1.2 Characterization of the expression levels of key metabolic enzymes and transporters during lung development

To determine the expression levels of enzymes and transporters of glucose catabolism during chick lung development, *in vitro* lung explant culture was performed. Briefly, this *ex vivo* system uses a nutritive medium and an air-liquid interface to mimic the *in vivo* lung growth, allowing the study of hypothetical molecular alterations that occur during lung branching. For this purpose, b1 to b3 lungs were processed for explant culture (as described in section 3.5) and incubated for 48 hours. Lung explants were collected, at D0 (0 hours) and at D2 (48 hours), to be analyzed by qRT-PCR for specific metabolic enzymes and transporters from glucose catabolism.

Specific primers were designed for *glut3*, *hk1*, *ldha*, *ldhb*, *pdha* and *pdhb* (and *18s* and *actin-β* as housekeeping genes). All fragments were amplified by conventional PCR, using cDNA from HH24 embryos and b2 lungs (table 2, section 3.7). Afterwards, fragments were analyzed by agarose gel electrophoresis. All the genes were present, both in the whole embryo and in the embryonic lung (Figure 10).

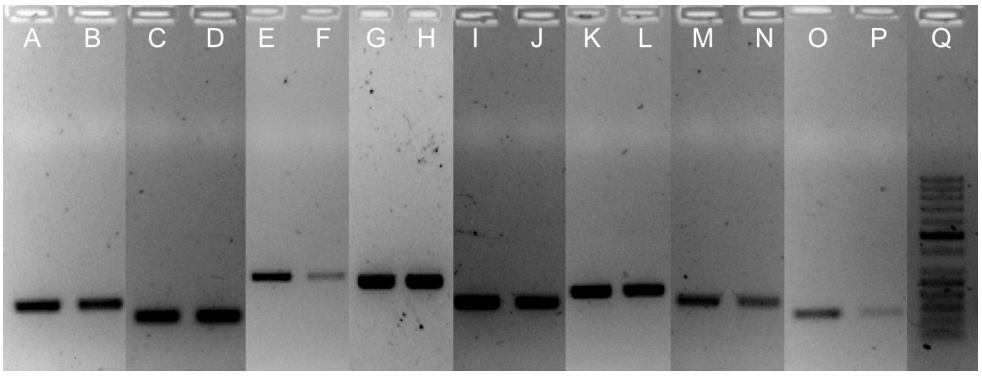

Figure 10 – Detection of amplified fragments by agarose gel electrophoresis. The fragments correspond to: *18s* (A-B), *actin-β* (C-D), *ldha* (E-F), *ldhb* (G-H), *pdha* (I-J), *pdhb* (K-L), *hk1* (M-N), *glut3* (O-P) and molecular weight size ladder (Q). For each gene the first band corresponds to the HH24 embryo and the second to the stage b2 lung, respectively.

4.1.3 mRNA expression levels of selected glucose catabolism molecular machinery at 0 hours

Figure 11 represents the relative expression levels of *glut3*, *hk1*, *ldha*, *ldhb*, *pdha* and *pdhb*, at 0 hours (expression levels were normalized for *18s* and *actin-β*). These genes are expressed in b1, b2 and b3 lungs, however, there are no statistical significant differences between the three stages, in any of the genes analyzed (Fig. 11a-f).

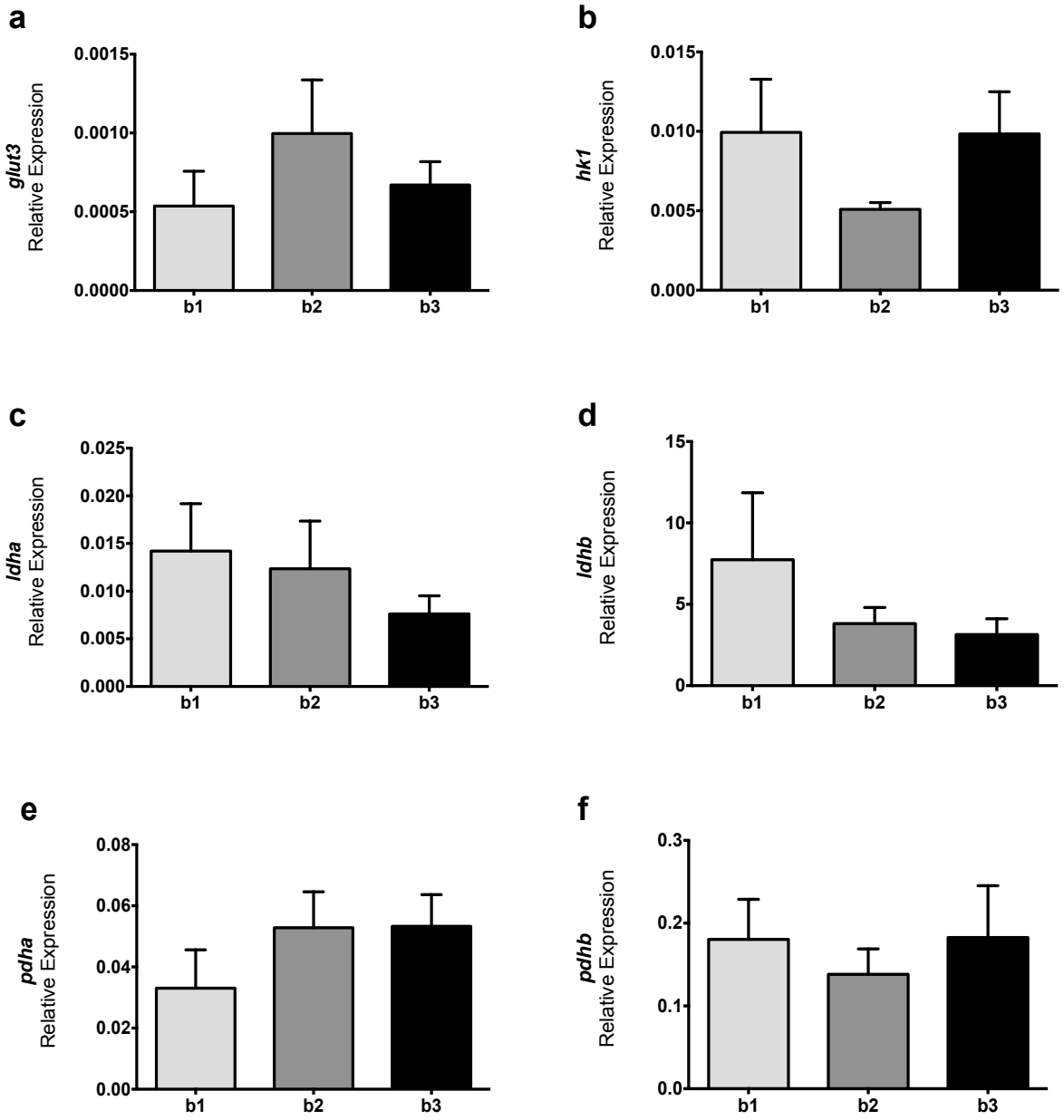

Figure 11 – mRNA expression levels of key glucose metabolism-related genes, at 0 hours. Representation of relative expression levels of *glut3* (a), *hk1* (b), *ldha* (c), *ldhb* (d), *pdha* (e) and *pdhb* (f) in b1, b2 and b3 lungs. Results are expressed as mean ± SEM (n=6/condition). Significantly different results ($p<0.05$).

4.1.4 mRNA expression levels of selected glucose catabolism molecular machinery at 48 hours

In Figure 12 are represented the relative expression levels of *glut3*, *hk1*, *ldha*, *ldhb*, *pdha* and *pdhb* at 48 hours (expression levels normalized for *18s* and *actin-β*). The gene expression levels were assessed at 48 hours (D2) and represented as fold variation to control, 0 hours (D0), in order to follow the mRNA variations throughout chick lung branching.

glut3 mRNA levels (Fig. 12a) present an increase in b1 stage (13.3 ± 4.2) in comparison to 0 hours. Throughout lung development, *glut3* expression levels decrease, in terms of fold variation, with statistical significant differences between b1 (13.3 ± 4.2) and b2 (6.1 ± 3.4), and between b2 and b3 (1.3 ± 0.2). *hk1* expression levels in b2 stage (3.1 ± 0.9) increase drastically when compared to 0 hours (Fig. 12b). From b1 (1.4 ± 0.3) to b2 is possible to verify a fold variation increase whereas from b2 to b3 stage *hk1* expression decreases (0.5 ± 0.2).

ldha mRNA levels (Fig. 12c) present a statistical significant increase in b1 (5.8 ± 2.0) and b3 (5.9 ± 0.8) when compared to 0 hours. Moreover, there is a fold variation decrease from b1 (5.8 ± 2.0) to b2 (2.6 ± 0.4). Then, in b3 lungs (5.9 ± 0.8) the expression level increases again. The relative expression of *ldhb* (Fig. 12d) does not show differences between the three groups, in terms of fold variation. Yet, b1 (0.2 ± 0.1), b2 (0.3 ± 0.1) and b3 (0.2 ± 0.1) lungs present a fold variation decrease from 0 hours.

Regarding *pdha*, no differences were detected in the three stages (Fig. 12e). Finally, *pdhb* (Fig. 12f) displays an increase in b1 (2.3 ± 0.7) when compared to 0 hours. Moreover, *pdhb* expression decreases, in fold variation, during lung development with a significant decrease from b1 to b3 (0.3 ± 0.02).

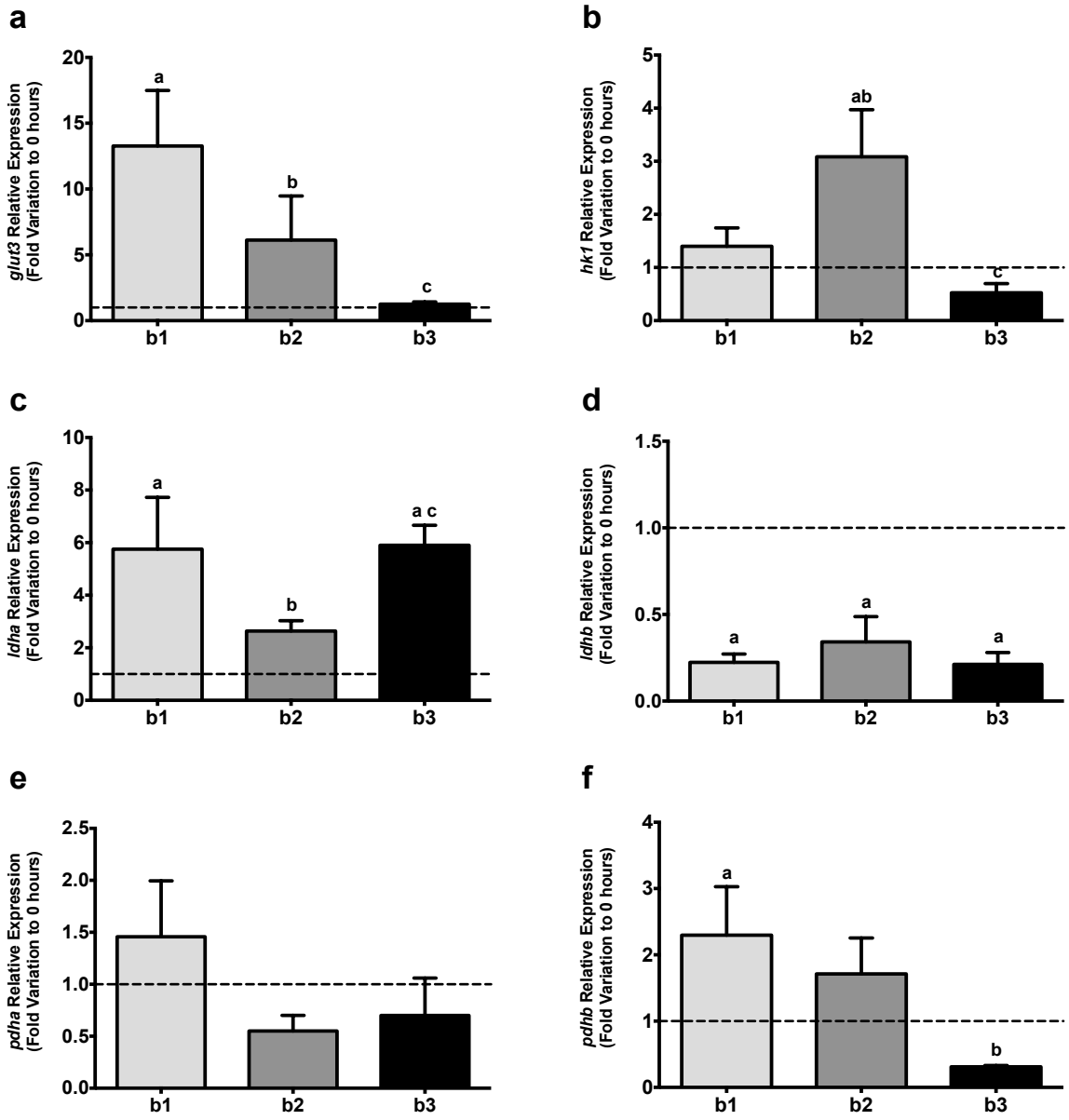

Figure 12 – mRNA expression levels of key glucose metabolism-related genes, at 48 hours. Representation of the relative expression levels, in fold variation, of the following genes: *glut3* (a), *hk1* (b), *ldha* (c), *ldhb* (d), *pdha* (e) and *pdhb* (f), when compared to 0 hours (dotted line). Results are expressed as mean ± SEM (n=6/condition). Significantly different results ($p<0.05$) are indicated as: a *vs* 0 hours; b *vs* b1; c *vs* b2.

4.1.5 Characterization of metabolites fluctuations after 48 hours in culture

To describe the metabolic alterations during chick lung development, *in vitro* lung explant culture was performed. With this system, it is possible to assess the extracellular metabolite fluctuations associated with chick lung branching. For this purpose, b1 to b3 lungs were processed for explant culture (as described in section 3.5) and incubated for 48 hours. While lung explants tissue was collected to be analyzed by qRT-PCR (previous section), the medium was stored, at D0 (0 hours), D1 (24 hours) and at D2 (48 hours), to be analyzed by ^{1}H-NMR spectroscopy. In this analysis, glucose and resultant metabolites from glucose catabolism namely, alanine, lactate and acetate were assessed. The metabolite data at 48 hours corresponds to the sum of data collected at 24 and 48 hours. The metabolite fluctuations were normalized taking into consideration the size of the explant. The lung epithelium perimeter is an excellent parameter to assess lung size, and the ratio D0/D2 is accepted as a lung growth measurement (described in section 3.6). In this case, results are expressed as the ratio between the amount of metabolites detected in the medium (in pmol) per growth ratio (the ratio between lung epithelial perimeters D2/D0).

The ^{1}H-NMR results revealed that glucose consumption (Fig. 13a) has similar values in the three stages studied (around 6 x 10^{5} pmol/growth ratio), implying a constant consumption as lung development proceeds. In what concerns alanine production (Fig. 13b), there are no statistical significant differences between b1, b2 and b3 lungs, after 48 hours in culture. Lactate production (Fig. 13c) displays an increase that accompanies chick lung development. Indeed, lactate production increases from stage b1 (3.0 x 10^{5} $\pm$ 6.2 x 10^{4} pmol/growth ratio) to b3 (4.5 x 10^{5} $\pm$ 1.7 x 10^{4} pmol/growth ratio). In addition, there is also an increase from b2 (3.3 x 10^{5} $\pm$ 3.7 x 10^{4} pmol/growth ratio) to b3. Finally, acetate production (Fig. 13d) augments throughout lung development, namely from stage b1 (3.6 x 10^{4} $\pm$ 5.1 x 10^{3} pmol/growth ratio) to stage b3 (5.9 x 10^{4} $\pm$ 2.4 x 10^{3} pmol/growth ratio).

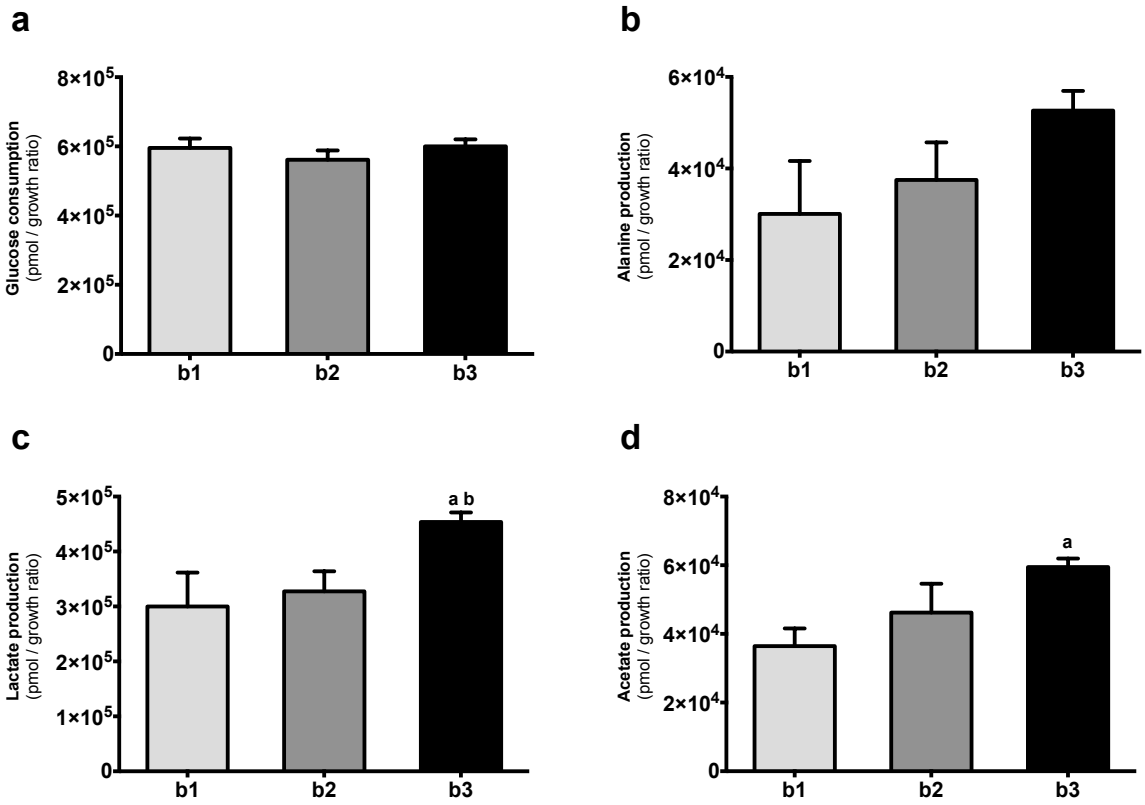

Figure 13 – Metabolite fluctuations during early stages of chick lung branching after 48 hours in culture. Representation of glucose consumption (a), alanine production (b), lactate production (c) and acetate production (d). Results are expressed as mean ± SEM (n=6/condition). Significantly different results ($p<0.05$) are indicated as: a *vs* b1; b *vs* b2.

4.2 Characterization of the RA-induced metabolism during early chick lung branching

Lung development is a complex process governed by epithelium-mesenchyme interactions and modulated by several transcription and growth factors, as for instance, RA. Retinoic acid modulates chick lung morphogenesis since it regulates branching and patterning. The cellular events underlying lung growth require high quantities of energy and carbon sources to form new cells. So, considering RA role in early lung branching, it is likely that it may modulate metabolic activity. For this reason, we sought to characterize the interactions between RA and metabolism, during early stages of lung development.

For this purpose, b2 lungs were processed for lung explant culture (as described in section 3.5) and incubated for 48 hours with 1 μM RA or with DMSO as control. Lung explants were collected and analyzed for *glut3*, *hk1*, *ldha*, *ldhb*, *pdha* and *pdhb* expression levels, by qRT-PCR. From the *in vitro* lung explant system, medium was collected and extracellular metabolites analyzed and quantified, by ^{1}H-NMR spectroscopy, namely: glucose, in order to study its consumption; the three major destinations of pyruvate such as alanine, lactate and acetate that comes from acetyl-CoA; pyruvate as a central metabolic intermediate; glutamine and glutamate as possible carbon suppliers of Krebs cycle. With this approach, extracellular metabolite fluctuations and alterations, at the expression levels, of glucose catabolism machinery associated with RA-induced metabolism during early chick lung branching, were assessed.

4.2.1 Impact of RA on the expression levels of key metabolic enzymes and transporters

To study the impact of RA on the expression levels of specific enzymes and transporters from glucose catabolism, qRT-PCR was performed for the following genes: *glut3*, *hk1*, *ldha*, *ldhb*, *pdha* and *pdhb* (expression levels were normalized for *18s* and *actin-β*). The expression levels were assessed, at 48 hours and compared between the two groups: 1 μM RA or DMSO as control.

glut3 mRNA levels in b2 lungs (Fig. 14a) are not affected by RA supplementation. Additionally, *hk1* transcript levels (Fig. 14b) show no differences among the groups. RA supplementation elicits an increase in *ldha* expression levels (Fig. 14c) (0.023 ± 0.007 relative expression) when compared to DMSO (0.005 ± 0.0005 relative expression). On other hand, there are no differences between the groups in *ldhb* mRNA levels (Fig. 14d). Both *pdha* (Fig. 14e) and *pdhb* (Fig. 14f) expression levels were not affected by RA supplementation.

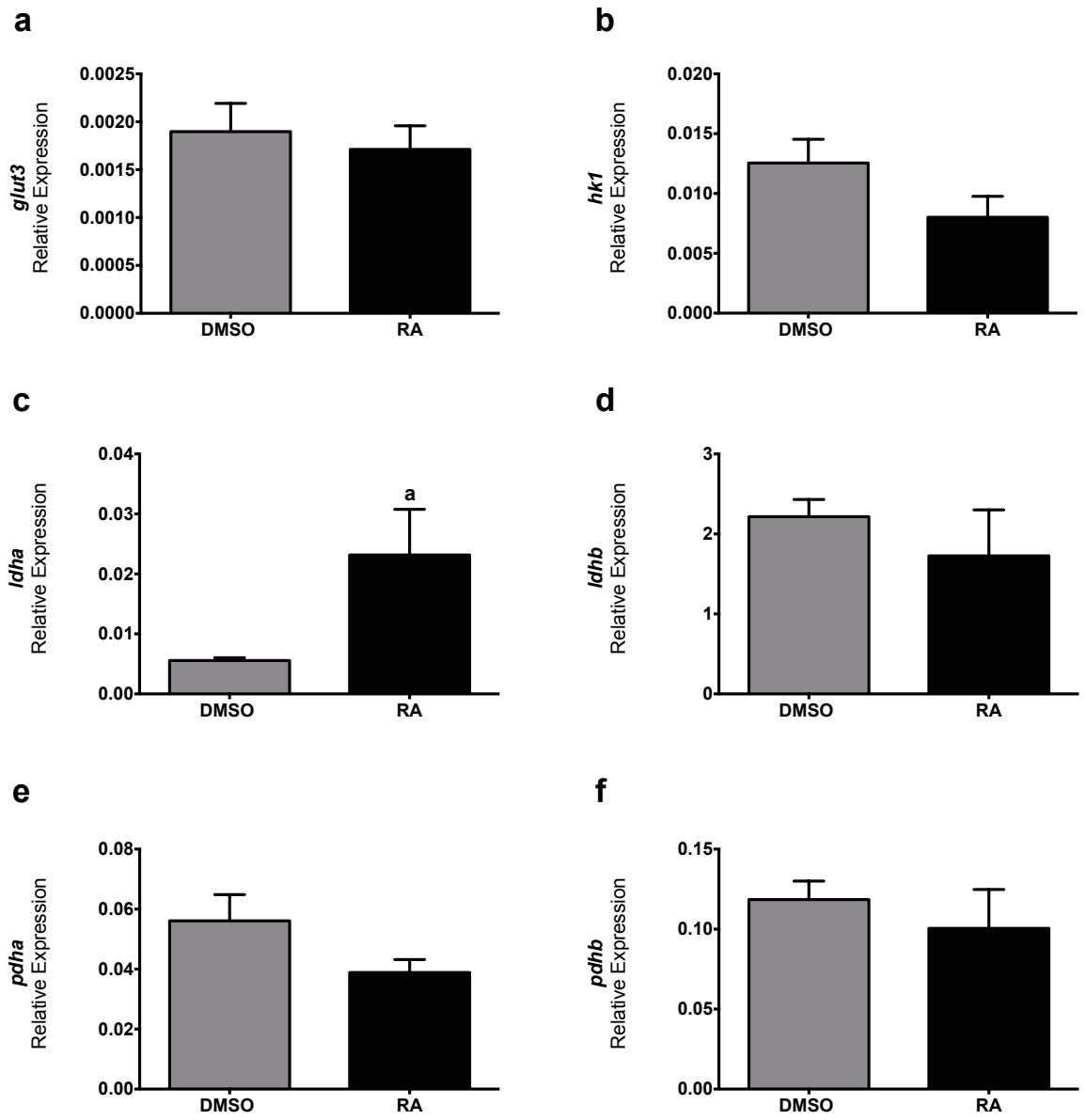

Figure 14 – mRNA expression levels of key glucose metabolism-related genes, after 48 hours, supplemented with 1 μM RA or DMSO. Representation of relative expression levels of *glut3* (a), *hk1* (b), *ldha* (c), *ldhb* (d), *pdha* (e), and *pdhb* (f). Results are expressed as mean ± SEM (n=6/condition). Significantly different results ($p<0.05$) are indicated as: a *vs* DMSO.

4.2.2 Impact of RA on metabolites fluctuations after 48 hours in culture

To characterize the impact of RA on the chick lung metabolism, b2 lungs were processed for lung explant culture (as described in section of 3.5) and incubated for 48 hours with 1 μM RA or with DMSO as control. The medium was collected, at D0 (hours), D1 (24 hours) and at D2 (48 hours), to be analyzed by ^{1}H-NMR spectroscopy, the metabolite data at 48 hours corresponds to the sum of data collected at 24 and 48 hours. In this analysis, glucose and resulting metabolites from glucose catabolism namely, alanine, lactate, acetate, pyruvate, glutamate and glutamine were assessed. The metabolite fluctuations were normalized taking into consideration the size of the explant, as previously described (section 4.1.5). Results are expressed as pmol per growth ratio.

The ^{1}H-NMR results revealed that RA induces a decrease in glucose consumption when comparing DMSO ($2.6 \times 10^{5} \pm 3.5 \times 10^{4}$ pmol/growth ratio) to RA group ($1.37 \times 10^{5} \pm 2.2 \times 10^{4}$ pmol/growth ratio) (Fig. 15a). Regarding alanine, RA decreases its production from $3.4 \times 10^{4} \pm 3.5 \times 10^{3}$ pmol/growth ratio to $2.4 \times 10^{4} \pm 1.4 \times 10^{3}$ pmol/growth ratio (Fig. 15b). Lactate production also decreases from DMSO ($4.3 \times 10^{5} \pm 8.2 \times 10^{4}$ pmol/growth ratio) to RA supplementation group ($2.7 \times 10^{5} \pm 2.9 \times 10^{4}$ pmol/growth ratio) (Fig. 15c). No differences were observed in acetate production (Fig. 15d). On the other hand, pyruvate production increase from $3.4 \times 10^{3} \pm 3.8 \times 10^{2}$ pmol/growth ratio in DMSO group, up to $6.1 \times 10^{3} \pm 7.7 \times 10^{2}$ pmol/growth ratio, with RA supplementation (Fig. 15e). Both glutamate and glutamine consumption remain unaltered (Fig. 15f and 15g, respectively).

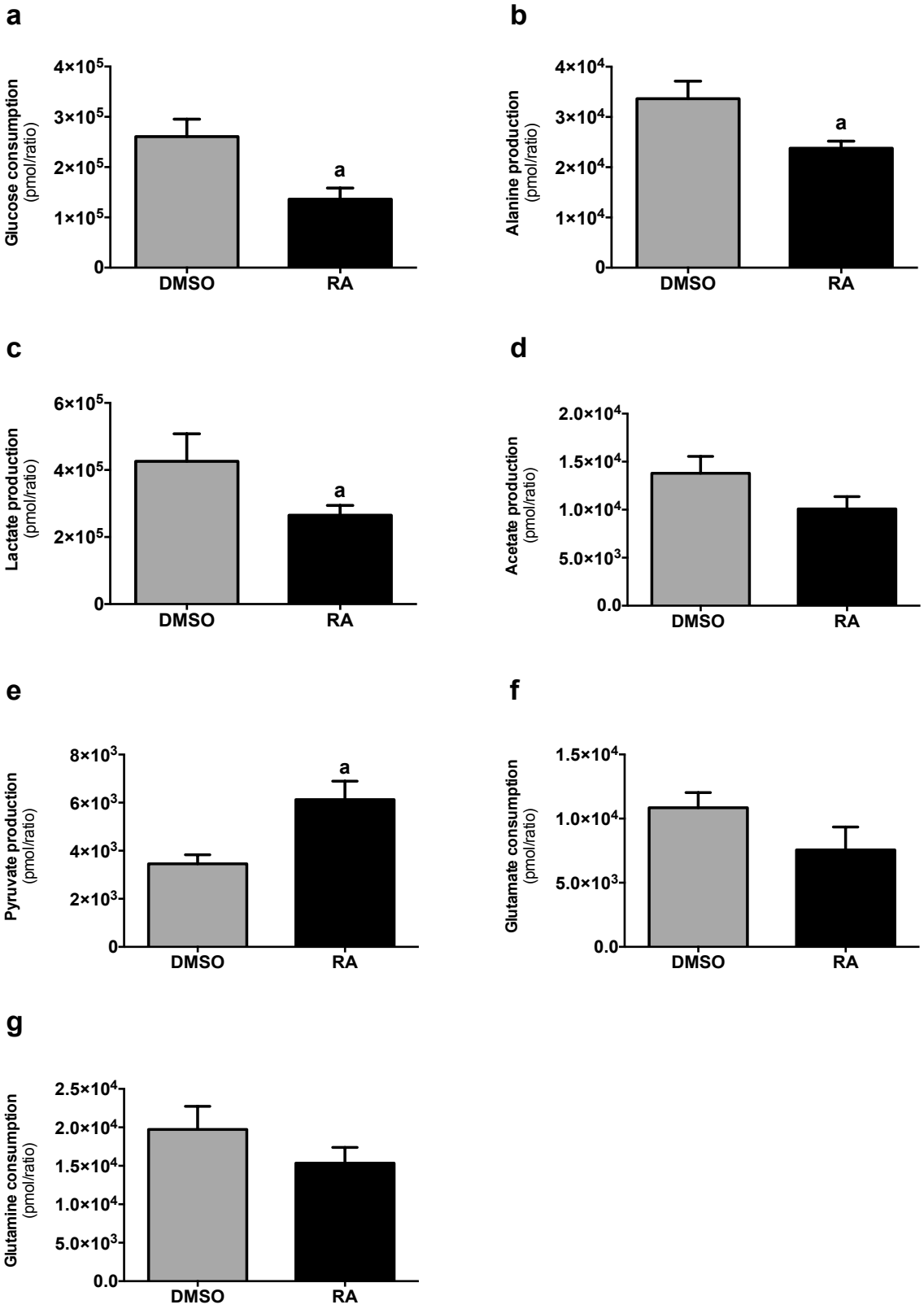

Figure 15 – Metabolite fluctuations of b2 lungs, after 48 hours in culture, under RA conditions. Representation of glucose consumption (a), alanine production (b), lactate production (c), acetate production (d), pyruvate production (e), glutamate consumption (f) and glutamine consumption (g). Results are expressed as mean ± SEM (n=6/condition). Significantly different results ($p<0.05$) are indicated as: a *vs* DMSO.

5. Discussion

Lung development is a complex process that depends on conserved signaling cascades working in cooperation to maintain numerous cellular processes, namely proliferation, differentiation, apoptosis and migration. Indeed, during branching morphogenesis, the pulmonary metabolic needs are supposedly enhanced since high amounts of energy and nutrients are required to support lung growth. The different metabolic pathways must be able to supply enough fuel to the tissue, and may be modulated by several transcription and growth factors to fulfil these requirements. Actually, the adult lung is a very active metabolically organ, and performs many functions such as clearance of the air, secretion of substances and gas-exchange, just to mention a few. The metabolic profile of the adult pulmonary system was widely studied in the 70´s and 80´s, and findings suggested a strong contribution from glucose catabolism in addition to a pronounced capacity for lipid biosynthesis. Nonetheless, the metabolic profile of the developing lung remains unknown. The work presented in this Master thesis addresses the metabolic processes associated with chick lung branching and the impact of retinoic acid, a well-known stimulator of lung morphogenesis, on lung metabolic profile. This study describes early lung metabolic biomarkers that might unravel new therapeutic strategies for lung disorders treatment.

5.1 Characterization of the metabolic profile of early chick lung branching

Adult lung metabolism relies on glucose utilization (von Wichert, 1972; Basset & Fisher, 1976a). Glucose oxidation represents a major source of energy and a crucial metabolic substrate for animals. Indeed, glucose uptake and catabolism are essential for all cellular processes, and are supposed to be enhanced in systems with high proliferative rates such as cancer and embryonic systems (Ito et al., 1999). In order to study the expression pattern and levels of crucial enzymes and transporters from glucose catabolism, embryonic chick lungs from b1, b2 and b3 stages were analyzed by *in situ* hybridization and qRT-PCR, respectively. With these two techniques, it was possible to obtain a semi-quantitative analysis and spatial distribution of specific transcripts, combined with an absolute quantitative method that shows the global amount of expression within the tissue. In this work the expression patterns and levels of *glut3*, *hk1*, *ldha*, *ldhb*, *pdha*, and *pdhb* were characterized, for the first time, in the embryonic chick lung.

5.1.1 Enzymes and transporters from glucose catabolism are expressed at early stages of chick lung branching

Glucose cellular uptake is made through specific carriers, namely glucose transporters (GLUTs), which consist of integral membrane glycoproteins that are able to transport glucose to the interior of the cells, by facilitated diffusion. This mechanism depends on the glucose gradient and it is limited by the number of transporters expressed in the cell surface. During chick lung development, *glut3* expression is stage-dependent, since it is absent in b1, but strongly expressed in b2 and b3 stages (Fig. 7a-c). *glut3* mRNA is present in the proximal region of the lung, namely in the tracheal mesenchyme (Fig. 7b) and expands distally from b2 to b3 (Fig. 7b and 7c, respectively). Furthermore, it is completely absent from the main bronchus epithelium, but present in the secondary bronchi (Fig. 7d). qRT-PCR revealed the presence of *glut3* transcripts, at 0 hours (which corresponds to the *in situ* hybridization timepoint), in the three stages studied and without significant statistical differences among the three groups (Fig. 11a). The lack of expression of *glut3* in b1 stage in *in situ* hybridization may be explained by the fact that this technique is less sensitive than qRT-PCR. In fact, the presence of *glut3* was previously described in chicken embryo fibroblasts and it has been suggested that it may be influenced by oncogenes and mitogens (Wastagaff et al., 1995). Moreover, *glut3* is highly expressed in the brain of adult broiler chickens (Kono et al., 2005). In the mammals, *glut3* transcripts are described as being present in the mesenchymal lung cells of tumors (Masin et al., 2015). Regarding the early chick lung, *glut3* is present mostly in the mesenchymal compartment and expands distally throughout development. *glut3* spatial distribution indicate that it may have an active role in glucose uptake in this cellular compartment and eventually in the secondary bronchi.

Once inside the cell, glucose is metabolized in a process named glycolysis. The first step is the activation of glucose through phosphorylation on carbon number 6, to produce glucose-6-phosphate. In fact, this reaction is one of the key regulatory points of glycolysis, and it is accomplished by an irreversible enzymatic reaction catalyzed by hexokinase, which transfers the phosphate group from ATP. In the chick embryonic lung, *hk1* expression pattern is conserved in b1, b2 and b3 lungs. *hk1* transcripts are mainly present in the mesenchymal compartment, namely in the trachea region (Fig. 7e) and in the dorsal mesenchyme (Fig. 7g). qRT-PCR revealed the presence of *hk1* expression in the three stages, but without statistical significant differences in its levels (Fig. 11b). According to these results, *hk1* is present in the mesenchymal compartment and its distribution matches *glut3* expression pattern in b2 and b3 stage,

suggesting that glucose, in the early chick lung, is handled in the mesenchymal compartment. In the epithelial compartment, most probably there are other GLUTs active to support glucose uptake.

Afterwards, glucose-6-phosphate suffers a series of metabolic steps until is transformed into pyruvate. Actually, only 5% of the chemical energy of glucose is released during glycolysis, which means that the remaining 95% of energy is still in the two resultant pyruvate molecules. On its turn, pyruvate can serve many destinations, among them to be utilized in alanine synthesis, to be diverted for lactate production or to serve as substrate for acetyl-CoA production. The first two enzymatic reactions are reversible and the last irreversible. Taking this into consideration, we decide to explore the expression pattern and levels of lactate and pyruvate dehydrogenases.

Lactate dehydrogenase is responsible for catalyzing the reduction of pyruvate into lactate, and this reaction is reversible. In the embryonic chick lung, *ldha* transcript is present in the trachea both in the mesenchymal and epithelial compartments (Fig. 8d). In the distal region of the lung, there is no *ldha* expression, namely in the main bronchus epithelium or secondary bronchi (Fig. 8c), but it is expressed in the mesenchyme of the tip (Fig. 8a). The expression levels remained unaltered in b1, b2 and b3, confirming the presence of *ldha* throughout development (Fig. 11c). On the other hand, *ldhb* expression pattern shows a completely different spatial distribution, because it is completely absent from the proximal region of the lung (Fig, 8e), but strongly expressed in the mesenchyme surrounding the distal tip (Fig, 8h). Moreover, *ldhb* is strongly expressed in the secondary bronchi (Fig. 8g). On the other hand, the expression levels revealed *ldhb* presence in all embryonic stages and without significant differences (Fig. 11d). These results clearly suggest a role for *ldha* mainly in the proximal region of the lung whereas *ldhb* will most likely be more relevant in the growing tips of the lung, namely in the tip of the main bronchi and also in the secondary buds.

The pyruvate dehydrogenase complex is responsible for pyruvate decarboxylation into acetyl-CoA, in an irreversible reaction. In the chick embryonic lung, *pdha* transcripts are present in the main bronchus mesenchyme and trachea (Fig. 9a-c). Moreover, *pdha* is highly expressed in the secondary bronchi (Fig. 9d). qRT-PCR revealed that *pdha* expression levels do not vary among the three stages (Fig. 11e). On the other hand, *pdhb* was detected by qRT-PCR without significant differences in b1, b2 and b3 stages (Fig. 11f). However, *pdhb* expression was not identified by *in situ* hybridization (Fig. 9e-g). This result is unexpected and may be explained if the antisense mRNA probe had not been properly designed, which needs further confirmation. In this sense, new primers will be designed to make a new probe. Both *pdha* and *pdhb* are to be present in the embryonic chick lung and *pdha* restricted to the mesenchymal compartment and secondary buds.

Briefly, pivotal enzymes and transporters from glucose catabolism are expressed at early stages of chick lung development and they are mainly confined to the mesenchymal compartment, among them *glut3*, *hk1*, *ldhb* and *pdha*. On the other hand, *ldha* is present in both epithelial and mesenchymal compartment. Regarding *pdhb*, it was not possible to assess its expression pattern, although qRT-PCR confirmed its presence in the chick lung. This feature sustains the hypothesis that, in the chick embryonic lung, glucose catabolism is confined to the mesenchymal compartment. Even so, metabolic products and energy resultant from these metabolic mechanisms can hypothetically be used for epithelium growth. In what concerns branching morphogenesis, *glut3*, *ldhb* and *pdha* are present in regions of active branching, such as the secondary bronchi and might contribute to support these embryonic structures in terms of energy and biomass.

5.1.2 Lactate and acetate are biomarkers of later stages of chick lung branching

After confirming the presence of glucose catabolism molecular machinery, the metabolite fluctuations that occur during chick lung branching were analyzed. For this purpose, b1 to b3 lungs were processed for explant culture and incubated for 48 hours. The culture medium was collected, at D0 (0 hours), D1 (24 hours) and at D2 (48 hours), to be analyzed by ^{1}H-NMR spectroscopy. The metabolite data at 48 hours corresponds to the sum of data collected at 24 and 48 hours. Simultaneously, to assess the alterations of pivotal enzymes and transporters throughout lung development, lung explants were collected and the expression levels of *glut3*, *hk1*, *ldha*, *ldhb*, *pdha* and *pdhb* were assessed by qRT-PCR, and date presented as 48 hours-fold variation to 0 hours.

During *in vitro* chick lung branching, glucose consumption was maintained from b1 to b3 (Fig. 13a) with a concurrent decrease of *glut3* transcript levels (Fig. 12a). Furthermore, this phenomenon was accompanied by a decrease in *hk1* expression levels, in later stages of lung development, namely from b2 to b3 (Fig. 12b). These results suggest an increase in the glycolytic efficiency and loss of *glut3* importance. Indeed, the developing lung is actively growing and must cope with high proliferative rates and, consequently, more energy and nutrients requirements. In this case, the embryonic lung seems to adapt to a more efficient way of glucose utilization, or as it progresses through development, it may seek out alternative sources to obtain energy and biomass. The adult lung metabolic requirements are similarly described as being, at least in part, achieved through glucose catabolism (von Wichert, 1972; Basset & Fisher, 1976a). However, some evidences point to contributions from other sources such as lipids (Felts, 1964).

Following glucose catabolism, each molecule of glucose is metabolized into two molecules of pyruvate through a series of metabolic reactions involving numerous enzymatic steps. In this study, only the three primary destinations of pyruvate were selected, namely: the conversion into alanine, lactate production and finally acetate from acetyl-CoA. Throughout lung development alanine production remain unaltered in the three stages studied (Fig. 13b). In fact, in the adult pulmonary system, it is described that part of glucose carbons serve for alanine production through pyruvate transamination that can be used for protein biosynthesis (Yeager & Massaro, 1972). In the chick embryonic lung, alanine is being produced since this metabolite is accumulating in the extracellular medium, however without major variations with time.

On the opposite, lactate production increases throughout lung development, namely from b1 to b3 and from b2 to b3, respectively (Fig. 13c). This boost in lactate production was accompanied by variations in *ldha* and *ldhb* expression levels. In fact, *ldha* initially decreased from b1 to b2 and then increased from b2 to b3 (Fig. 12c). *ldhb* transcript levels remained unchanged thru development, but decreased from 0 to 48 hours (Fig. 12d). Interestingly, *ldha* expression is inversely related with *hk1*, since when one increases the other decreases, and this is verified in the three stages studied, suggesting a possible inter-regulation between the two enzymes encoded by these two genes. This increase in lactate production throughout embryonic development, suggests a shift to lactate production in detriment of mitochondrial respiration. Indeed, this metabolic alteration is accompanied by a decrease in total *ldh* expression levels, since *ldhb* seems to be much more expressed than *ldha*. This behavior could be related with a response, at the transcriptional level, to the amount of lactate that is accumulating inside the cell and, consequently, exported to the extracellular medium. A similar phenomenon happens in the adult lung, where almost 50% of the carbons from glucose are metabolized into pyruvate and lactate, and from this fraction, the lactate production is 10-fold higher than pyruvate (Basset & Fisher, 1975b).

Finally, acetate, that can be originated from acetyl-CoA, also increases its production in later stages of lung development, namely from b1 to b3 stage (Fig. 13d). This increment in the extracellular levels of acetate was accompanied by a decrease in terms of *pdhb* expression levels, namely from b1 to b3 (Fig. 12f). On the other hand, *pdha* expression levels, remained unaltered in the three stages studied (Fig. 12e). These data may indicate that pyruvate is being transformed into acetate through acetyl-CoA, supporting the impairment of Krebs cycle. Yet, the increase in the amount of extracellular acetate could also be related with the fact that this metabolite can be produced to be incorporated into the newly synthesized cellular membranes, which is quite common in systems with high cellular division rates.

Furthermore, acetate can be used for lipid biosynthesis similarly to what happens in the adult mammalian lung (Basset et al., 1981).

In general, lactate and acetate are increased in later stages of lung development with a concurrent metabolic shift from Krebs cycle to lactate production. In fact, lactate and acetate can be suggested as biomarkers of chick lung branching. Furthermore, branching morphogenesis seems to be accompanied by temporal metabolic changes (from stage b1 to stage b3) both in terms of metabolites fluctuations and genetic modulations. In figure 16, a schematic representation of the metabolic profile of chick lung branching is represented.

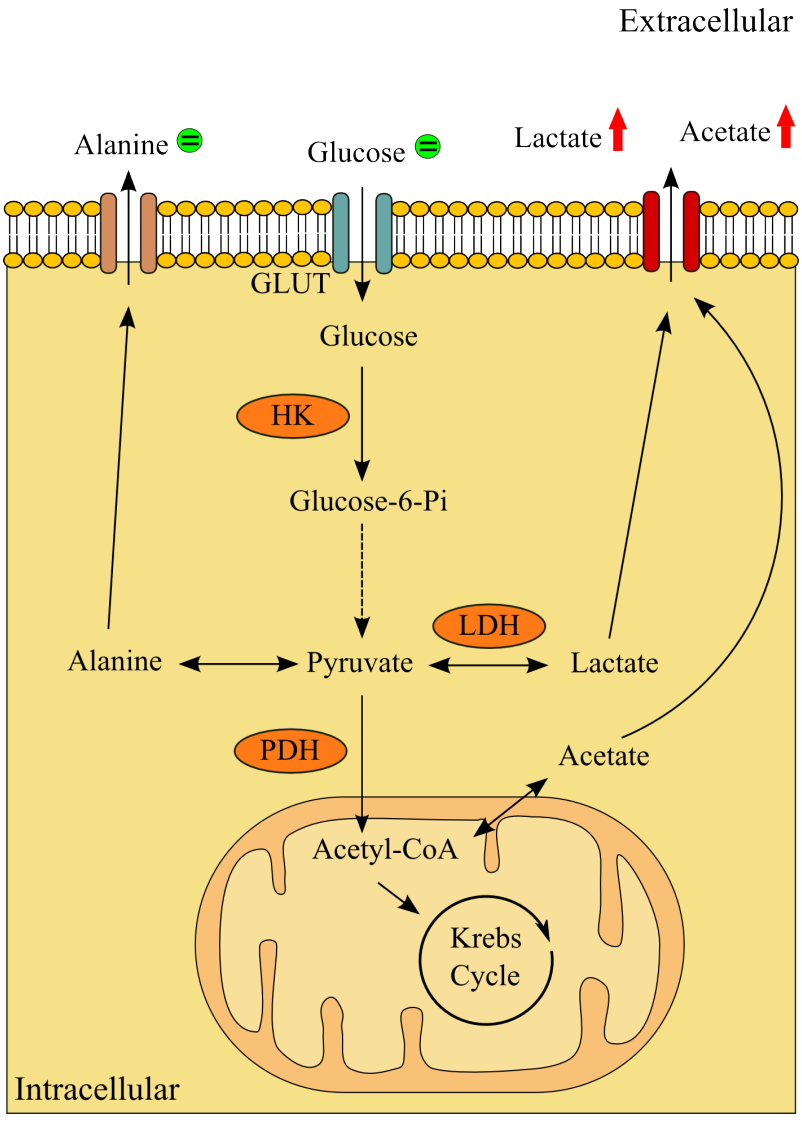

Figure 16 – Schematic representation of the metabolic profile of early stages of chick lung branching. The metabolites detected in the extracellular medium can either be consumed (glucose) or produced (alanine, lactate and acetate) by the lung tissue. The symbols refer to constant (=), increase (↑) or decrease (↓) in metabolites, considering their particular fate.

5.2 Characterization of the RA-induced metabolism of early chick lung branching

Retinoic acid is a well-known growth factor implicated in many cellular processes namely, proliferation, differentiation and apoptosis, thus contributing for the morphogenesis of different organs and systems. Indeed, RA functionality extends from the early embryo formation to the adult homeostasis. Recently, RA was described as a crucial molecular player for chick lung development by increasing branching in a dose-dependent manner. Moreover, it was implicated in a complex molecular network that contributes to branching morphogenesis and proximal-distal patterning of the embryonic chick lung (Fernandes-Silva et al., 2017). On the other hand, RA has been described as a potential metabolic modulator, associated with glucose, lipids and proteins metabolism modulation. In the current study, the hypothetical interactions between RA and the metabolic processes associated to branching morphogenesis of the chicken lung were dissected.

For this purpose, b2 lungs were processed for explant culture, supplemented with 1 μM of RA or DMSO, and incubated for 48 hours. The culture medium was collected, at D0 (0 hours), D1 (24 hours) and at D2 (48 hours), and the extracellular metabolites (glucose, alanine, lactate, acetate, pyruvate, glutamate and glutamine) analyzed by ^{1}H-NMR spectroscopy. The metabolite data at 48 hours corresponds to the sum of data collected at 24 and 48 hours. Simultaneously, to assess the alterations of pivotal enzymes and transporters throughout lung development, lung explants were collected and the expression levels of *glut3*, *hk1*, *ldha*, *ldhb*, *pdha* and *pdhb* evaluated by qRT-PCR.

5.2.1 RA induces major metabolic changes in chick lung branching

Retinoic supplementation, *in vitro*, induced a decrease in glucose consumption, in comparison with DMSO control group (Fig. 15a). However, in terms of expression, *glut3* and *hk1* transcript levels remained unaltered (Fig. 14a and b, respectively). Most probably RA influences the expression levels of other GLUTs than *glut3*, thus decreasing the total influx of glucose. In a similar way, alanine production decreased in RA-treated culture (Fig. 15b), most probably due to the reduction of the glycolysis subtract. The lactate production of b2 lungs was also decreased when compared to control (Fig. 15c), with a simultaneous increase of *ldha* expression levels whereas *ldhb* mRNA levels remained unchanged (Fig. 14c and 14d, respectively). The decline in lactate production may be a consequence of the reduction in the amount of glucose available to be metabolized. Moreover, once lactate dehydrogenase reactions can occur in the two directions, the increase regarding *ldha* expression may be associated with the necessity

to perform the reverse enzymatic reaction. Still, acetate production (Fig. 15d) did not show major differences between the RA-treated group and DMSO. To seek for alternative carbon sources, glutamine metabolism was also investigated. In fact, glutamine is able to supply the Krebs cycle through a bidirectional reaction that includes glutamate, which on its turn can be incorporated into α-Ketoglutarate. However, both glutamine and glutamate consumptions were unaffected by RA supplementation (Fig. 15f and 15g, respectively). Notwithstanding, pyruvate production had a major increase as consequence of RA treatment (Fig. 15e), although *pdha* and *pdhb* expression levels stay unaltered (Fig. 14e and 14f, respectively). In figure 17, a schematic representation of the RA-induced metabolism associated with chick lung branching is represented.

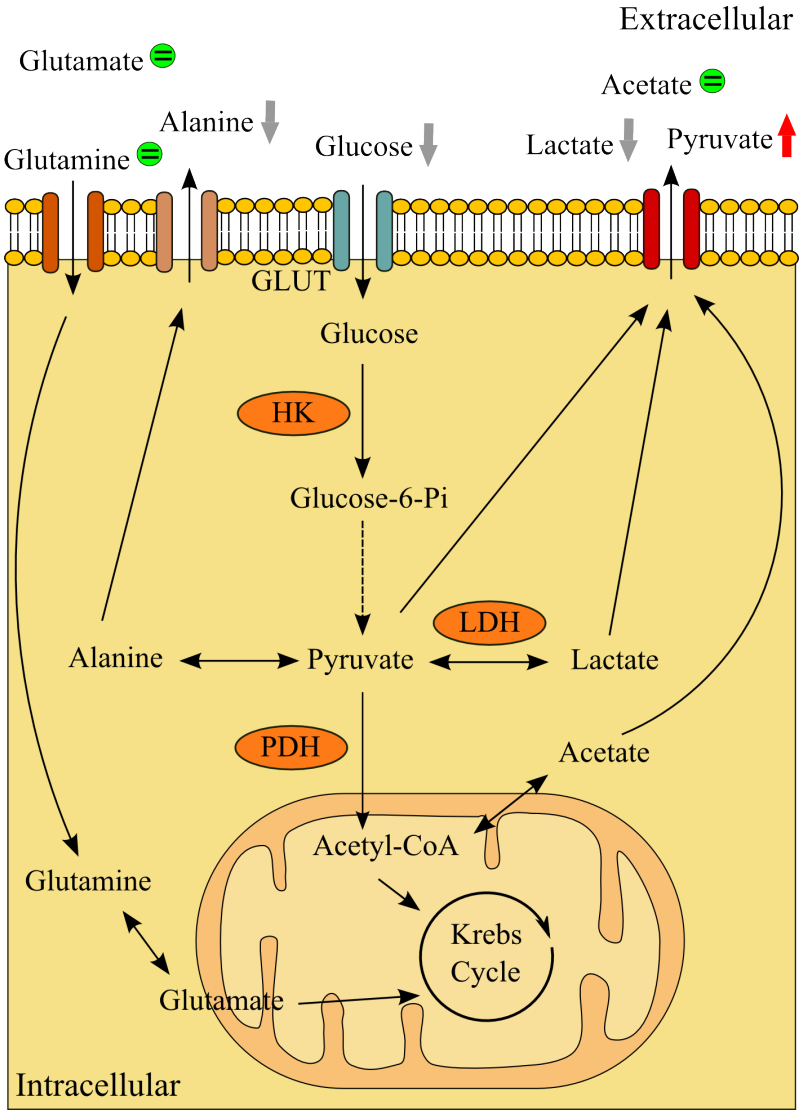

Figure 17 – Schematic representation of the RA-induced metabolism associated with chick lung branching. The metabolites detected in the extracellular medium can either be consumed (glucose, glutamate and glutamine) or produced (alanine, lactate, acetate and pyruvate) by the lung tissue. The symbols refer to constant (=), increase (↑) or decrease (↓) in metabolites, considering their particular fate, when compared to control conditions.

Taking into consideration that glucose consumption is reduced, lactate and alanine production is decreased while acetate production remained equal, it is likely that alternative pyruvate sources to glucose may exist, under the influence of RA. In view of these results, proteins and lipids are plausible candidates as pyruvate source, as well. In fact, lipids appear as a reliable way to supply the lung with pyruvate. In fact, the adult pulmonary tissue displays a pronounced capacity to oxidize fatty acids both from plasma lipoproteins and from free non-esterified fatty acids (Felts, 1964). In addition, and in opposition to the minimal glucose reserves, the lipid lung storage is more than sufficient to supply the lung metabolic requirements, via lipid oxidation, in the adult lung (Tierney, 1974). Furthermore, the adult pulmonary system requires high lipid biosynthesis rates to produce the lung surfactant. This fluid is crucial for reducing the surface tension of the air-liquid interface and increases the elasticity compliance of the terminal airways to avoid the alveolar collapse. Indeed, surfactant fluid composition relies on 90% of lipid content (Veldhuizen et al., 1998), and curiously other species which do not exhibit alveoli, such as birds, also depend on surfactant fluid, suggesting additional functions for this fluid (Bernhard et al., 2001), namely a nutritional one.

Similarly, in the embryonic chick lung, during branching morphogenesis, lipids are a strong candidate to supply the production of pyruvate. Here, we hypothesize that RA treatment is promoting a shift in the metabolic profile of early chick lung to an adult-like lung metabolic profile. In fact, in the culture medium used, the *in vitro* explant system is composed, among other constituents, by serums that are known to be rich in lipids. Furthermore, and according to the literature, RA has been described as a potential lipid metabolic modulator by promoting changes in lipid oxidation, biosynthesis and storage (Amengual et al., 2010). Yet, RA modulates mitochondria biogenesis and function both in liver and adipocyte systems, by influencing a great number of genes related with oxidative phosphorylation (Tourniaire et al., 2015). Further studies are necessary to clarify and characterize the impact of RA on early stages of the chick lung branching metabolic profile.

6. Conclusions and Future Perspectives

Lung development is a complex process dependent on the activation of conserved signaling pathways that regulate pivotal cellular processes such as proliferation, differentiation, apoptosis and migration. It is widely accepted that these cellular events require high amounts of energy and nutrients to form new biomass. However, the metabolic changes that occur during chick lung branching have not been described so far. Moreover, RA is a crucial growth factor that has being implicated in early branching morphogenesis of the chick lung and involved in a molecular network that modulates this event in a dose-dependent manner. RA is also suggested as a modulator of several metabolic processes. Nonetheless, the interactions between RA and lung branching metabolism are still unknown.

In this study, we described, for the first time, the temporal metabolic changes associated with chick pulmonary branching. Indeed, throughout lung development the glycolytic efficiency increases and Krebs cycle metabolism shifts to lactate production. In this context, acetate and lactate are seen as metabolic biomarkers of early lung development.

Additionally, we describe the impact of RA on branching morphogenesis metabolism. RA elicits extensive metabolic changes and, accordingly, prompted us to suggest that RA may shift the normal lung glucose-based metabolism to a metabolism where lipids are potentially seen as source of carbons and energy.

Further studies will be needed to unveil additional mechanisms by which RA interacts with the metabolism of the chick lung branching. The exploration and characterization of this association, during embryonic lung development, more precisely during branching morphogenesis could be of great importance to reveal novel therapeutic approaches that eventually contribute to treating lung disorders.

In terms of future perspectives, it will be of great value to explore the contribution of other GLUTs such as *glut1*, *glut2* and *glut8*, which are described as being present in the chicken. Moreover, lactate and acetate metabolism in the early chick lung, should be examined, namely regarding monocarboxylate transporters (MCTs). Regarding RA-induced metabolism, it will be of great importance to explore the contribution of lipids and its metabolism for chick lung branching. Furthermore, since RA has major impact on the genetic aspects of mitochondria and oxidative phosphorylation this should be examined, in the context of lung development.

7. References

Alves, M.G., Neuhaus-Oliveira, A., Moreira, P.I., Socorro, S., & Oliveira, P.F. (2013). Exposure to 2,4-dichlorophenoxyacetic acid alters glucose metabolism in immature rat Sertoli cells. *Reprod Toxicol*, *38C*, 81-88. doi:10.1016/j.reprotox.2013.03.005

Alves, M.G., Oliveira, P.F., Martins, F.O., Oliveira, P.J., & Carvalho, R.A. (2012). Gender-dependent Metabolic Remodeling During Heart Preservation in Cardioplegic Celsior and Histidine Buffer Solution. *J Cardiovasc Pharmacol*, *59*, 151-157. doi:10.1097/FJC.0b013e3182391d17

Amengual, J., Ribot, J., Bonet, M.L., & Palou, A. (2008). Retinoic acid treatment increases lipid oxidation capacity in skeletal muscle of mice. *Obesity (Silver Spring)*, *16*(3), 585-591. doi:10.1038/oby.2007.104

Amengual, J., Ribot, J., Bonet, M.L., & Palou, A. (2010). Retinoic acid treatment enhances lipid oxidation and inhibits lipid biosynthesis capacities in the liver of mice. *Cell Physiol Biochem*, *25*(6), 657-666. doi:10.1159/000315085

Balkissoon, R., Lommatzsch, S., Carolan, B., & Make, B. (2011). Chronic obstructive pulmonary disease: a concise review. *Med Clin North Am 95*(6), 1125-1141. doi:10.1016/j.mcna.2011.08.009

Bassett, D.J., & Fisher, A.B. (1976a). Metabolic response to carbon monoxide by isolated rat lungs. *Am J Physiol*, *230*, 658-663.

Bassett, D.J., & Fisher, A.B. (1976b). Pentose cycle activity of the isolated perfused rat lung. *Am J Physiol*, *231*, 1527-1532.

Bassett, D.J., Hamosh, M., Hamosh, P., & Rabinowitz, J.L. (1981). Pathways of palmitate metabolism in the isolated rat lung. *Exp Lung Res*, *2*, 37-47. doi:10.3109/01902148109052301

Batten, M.L., Imanishi, Y., Maeda, T., Tu, D.C., Moise, A.R., Bronson, D., Possin, D., Van Gelder, R.N., Baehr, W., & Palczewski, K. (2004). Lecithin-retinol acyltransferase is essential for accumulation of all-trans-retinyl esters in the eye and in the liver. *J Biol Chem*, *279*(11), 10422-10432. doi:10.1074/jbc.M312410200

Bellairs, R., & Osmond, M. (2014). Atlas of Chick Development (3rd Edition). Oxford: Academic Press.

Bernhard, W., Gebert, A., Vieten, G., Rau, G.A., Hohlfeld, J.M., Postle, A.D., & Freihorst, J. (2001). Pulmonary surfactant in birds: coping with surface tension in a tubular lung. *Am J Physiol Regul Integr Comp Physiol*, *281*(1), R327-337.

Berry, D.C., Jacobs, H., Marwarha, G., Gely-Pernot, A., O'Byrne, S.M., DeSantis, D., Klopfenstein, M., Feret, B., Dennefeld, C., Blaner, W.S., Croniger, C.M., Mark, M., Noy, N., & Ghyselinck, N.B. (2013). The STRA6 receptor is essential for retinol-binding protein-induced insulin resistance but

not for maintaining vitamin A homeostasis in tissues other than the eye. *J Biol Chem*, *288*(34), 24528-24539. doi:10.1074/jbc.M113.484014

Blomhoff, R., Helgerud, P., Rasmussen, M., Berg, T., & Norum, K.R. (1982). In vivo uptake of chylomicron [3H]retinyl ester by rat liver: evidence for retinol transfer from parenchymal to nonparenchymal cells. *Proc Natl Acad Sci U S A*, *79*(23), 7326-7330.

Cabrera-Valladares, G., Matschinsky, F.M., Wang, J., & Fernandez-Mejia, C. (2001). Effect of retinoic acid on glucokinase activity and gene expression in neonatal and adult cultured hepatocytes. *Life Sci*, *68*(25), 2813-2824. doi:10.1016/S0024-3205(01)01065-7

Cardoso, W.V., & Lü, J. (2006) Regulation of early lung morphogenesis: questions, facts and controversies. *Development*, *133*, 1611-1624. doi:10.1242/dev.02310

Cardoso, W.V., Williams, M.C., Mitsialis, S.A., Joyce-Brady, M., Rishi, A.K., & Brody, J.S. (1995). Retinoic acid induces changes in the pattern of airway branching and alters epithelial cell differentiation in the developing lung in vitro. *Am J Respir Cell Mol Biol*, *12*, 464-476. doi:10.1165/ajrcmb.12.5.7742011

Chambon, P. (1996). A decade of molecular biology of retinoic acid receptors. *FASEB J*, *10*(9), 940-954.

Chen, F., Cao, Y., Qian, J., Shao, F., Niederreither, K., & Cardoso, W.V. (2010) A retinoic acid–dependent network in the foregut controls formation of the mouse lung primordium. *J Clin Invest*, *120*(6), 2040-2048. doi:10.1172/JCI40253

Chen, F., Desai, T.J., Qian, J., Niederreither, K., Lü, J., & Cardoso, W.V. (2007) Inhibition of Tgf beta signaling by endogenous retinoic acid is essential for primary lung bud induction. *Development*, *134*(16), 2969-2979. doi:10.1242/dev.006221

Chen, G., Zhang, Y., Lu, D., Li, N.Q., & Ross, A.C. (2009). Retinoids synergize with insulin to induce hepatic Gck expression. *Biochem J*, *419*(3), 645-653. doi:10.1042/BJ20082368

Crow, J.A., & Ong, D.E. (1985). Cell-specific immunohistochemical localization of a cellular retinol-binding protein (type two) in the small intestine of rat. *Proc Natl Acad Sci U S A*, *82*(14), 4707-4711.

Cunningham, T.J., & Duester, G. (2015). Mechanisms of retinoic acid signalling and its roles in organ and limb development. *Nat Rev Mol Cell Biol*, *16*(2), 110-123. doi:10.1038/nrm3932

Davidson, L.M., & Berkelhamer, S.K. (2017). Bronchopulmonary Dysplasia: Chronic Lung Disease of Infancy and Long-Term Pulmonary Outcomes. *J Clin Med*, *6*(1), pii: E4. doi:10.3390/jcm6010004

Decaux, J.F., Juanes, M., Bossard, P., & Girard, J. (1997). Effects of triiodothyronine and retinoic acid on glucokinase gene expression in neonatal rat hepatocytes. *Mol Cell Endocrinol*, *130*(1-2), 61-67. doi:10.1016/S0303-7207(97)00074-9

Duester, G. (1998). Alcohol dehydrogenase as a critical mediator of retinoic acid synthesis from vitamin A in the mouse embryo. *J Nutr*, *128*(2 Suppl), 459S-462S.

Duester, G. (2008). Retinoic acid synthesis and signaling during early organogenesis. *Cell*, *134*(6), 921-931. doi:10.1016/j.cell.2008.09.002

During, A., & Harrison, E.H. (2007). Mechanisms of provitamin A (carotenoid) and vitamin A (retinol) transport into and out of intestinal Caco-2 cells. *J Lipid Res*, *48*(10), 2283-2294. doi:10.1194/jlr.M700263-JLR200

Esteban-Pretel, G., Marín, M.P., Cabezuelo, F., Moreno, V., Renau-Piqueras, J., Timoneda, J., & Barber, T. (2010). Vitamin A deficiency increases protein catabolism and induces urea cycle enzymes in rats. *J Nutr*,*140*(4), 792-798. doi:10.3945/jn.109.119388

Felts, J.M. (1964). Biochemistry of the Lung. *Health Phys*, *10*, 973-979.

Fernandes-Silva, H., Vaz-Cunha, P., Barbosa, V.B., Silva-Gonçalves, C., Correia-Pinto, J., & Moura, R.S. (2017) Retinoic acid regulates avian lung branching through a molecular network. *Cell Mol Life Sci*, in press. doi:10.1007/s00018-017-2600-3

Fex, G., & Johannesson, G. (1988). Retinol transfer across and between phospholipid bilayer membranes. *Biochim Biophys Acta*, *944*(2), 249-255. doi:10.1016/0005-2736(88)90438-5

Fisher, A.B. (1984). Intermediary metabolism of the lung. *Environ Health Perspect*, *55*, 149-158.

Gleghorn, J.P., Kwak, J., Pavlovich, A.L., & Nelson, C.M. (2012). Inhibitory morphogens and monopodial branching of the embryonic chicken lung. *Dev Dyn*, *241*(5), 852-862. doi:10.1002/dvdy.23771

Golzio, C., Martinovic-Bouriel, J., Thomas, S., Mougou-Zrelli, S., Grattagliano-Bessieres, B., Bonniere, M., Delahaye, S., Munnich, A., Encha-Razavi, F., Lyonnet, S., Vekemans, M., Attie-Bitach, T., & Etchevers, H.C. (2007). Matthew-Wood syndrome is caused by truncating mutations in the retinol-binding protein receptor gene STRA6. *Am J Hum Genet*, *80*(6), 1179-1187. doi:10.1086/518177

Goodman, D.S. (1980). Plasma retinol-binding protein. *Ann N Y Acad Sci*, *348*, 378-390. doi:10.1111/j.1749-6632.1980.tb21314.x

Graham, T.E., Yang, Q., Bluher, M., Hammarstedt, A., Ciaraldi, T.P., Henry, R.R., Wason, C.J., Oberbach, A., Jansson, P.A., Smith, U., & Kahn, B.B. (2006). Retinol-binding protein 4 and insulin resistance

in lean, obese, and diabetic subjects. *N Engl J Med*, *354*(24), 2552-2563. doi:10.1056/NEJMoa054862

Green, M.R., & Sambrook, J. (2012) Molecular Cloning. A Laboratory Manual (4th edition). New York: Spring Harbor Laboratory Press.

Hamburger, V., & Hamilton, H.L. (1951). A series of normal stages in the development of the chick embryo. *J Morphol*, *88*(1), 49-92.

Henrique, D., Adam, J., Myat, A., Chitnis, A., Lewis, J., & Ish-Horowicz, D. (1995). Expression of a Delta homologue in prospective neurons in the chick. *Nature*, *375*, 787-790. doi:10.1038/375787a0

Herriges, M., & Morrisey, E.E. (2014). Lung development: orchestrating the generation and regeneration of a complex organ. *Development*, *141*(3), 502-513. doi:10.1242/dev.098186

Hind, M., & Maden, M. (2004) Retinoic acid induces alveolar regeneration in the adult mouse lung. *Eur Respir J*, *23*(1), 20-27. doi:10.1183/09031936.03.00119103

Humphrey, B.D., Stephensen, C.B., Calvert, C.C., & Klasing, K.C. (2004) Glucose and cationic amino acid transporter expression in growing chickens (Gallus gallus domesticus). *Comp Biochem Physiol A Mol Integr Physiol*, *138*(4), 515-525. doi:10.1016/j.cbpb.2004.06.016

Ito, T., Noguchi, Y., Udaka, N., Kitamura, H., & Satoh, S. (1999) Glucose transporter expression in developing fetal lungs and lung neoplasms. *Histol Histopathol*, *14*(3), 895-904.

Kashyap, V., & Gudas, L.J. (2010). Epigenetic regulatory mechanisms distinguish retinoic acid-mediated transcriptional responses in stem cells and fibroblasts. *J Biol Chem*, *285*(19), 14534-14548. doi:10.1074/jbc.M110.115345

Kawaguchi, R., Yu, J., Honda, J., Hu, J., Whitelegge, J., Ping, P., Wiita, P., Bok, D., & Sun, H. (2007). A membrane receptor for retinol binding protein mediates cellular uptake of vitamin A. *Science*, *315*(5813), 820-825. doi:10.1126/science.1136244

Keller, R.L., Tacy, T.A., Hendricks-Munoz, K., Xu, J., Moon-Grady, A.J., Neuhaus, J., Moore, P., Nobuhara, K.K., Hawgood, S., & Fineman, J.R. (2010). Congenital diaphragmatic hernia: endothelin-1, pulmonary hypertension, and disease severity. *Am J Respir Crit Care Med*, *182*(4), 555-561. doi:10.1164/rccm.200907-1126OC

Kim, H.Y., Varner, V.D., & Nelson, C.M. (2013). Apical constriction initiates new bud formation during monopodial branching of the embryonic chicken lung. *Development*, *140*(15), 3146-3155. doi:10.1242/dev.093682

Kimura, J., & Deutsch, G.H. (2007). Key mechanisms of early lung development. *Pediatr Dev Pathol*, *10*(5), 335-347. doi:10.2350/07-06-0290.1

Klaus, M., Reiss, O.K., TOoOley, W.H., Peil, C., & Clements, J.A. (1962). Alveolar epithelial cell mitochondria as source of the surface-active lung lining. *Science*, *137*(3532), 750-761.

Kono, T., Nishida, M., Nishiki, Y., Seki, Y., Sato, K., & Akiba, Y. (2005). Characterisation of glucose transporter (GLUT) gene expression in broiler chickens. *Br Poult Sci*, *46*(4), 510-525. doi:10.1080/00071660500181289

Kumar, S., & Duester, G. (2014). Retinoic acid controls body axis extension by directly repressing Fgf8 transcription. *Development*, *141*(15), 2972-2977. doi:10.1242/dev.112367

Kumar, S., Sandell, L.L., Trainor, P.A., Koentgen, F., & Duester, G. (2012). Alcohol and aldehyde dehydrogenases: retinoid metabolic effects in mouse knockout models. *Biochim Biophys Acta*, *1821*(1), 198-205. doi:10.1016/j.bbalip.2011.04.004

Li, E., Norris, A.W. (1996). Structure/function of cytoplasmic vitamin A-binding proteins. *Annu Rev Nutr*, *16*, 205-234. doi:0.1146/annurev.nu.16.070196.001225

Liu, L., & Gudas, L.J. (2005). Disruption of the lecithin:retinol acyltransferase gene makes mice more susceptible to vitamin A deficiency. *J Biol Chem*, *280*(48), 40226-40234. doi:10.1074/jbc.M509643200

Lobo, G.P., Amengual, J., Baus, D., Shivdasani, R.A., Taylor, D., & von Lintig, J. (2013). Genetics and diet regulate vitamin A production via the homeobox transcription factor ISX. *J Biol Chem*, *288*(13), 9017-9027. doi:10.1074/jbc.M112.444240

Loscertales, M., Mikels, A.J., Hu, J.K., Donahoe, P.K., & Roberts, D.J. (2008). Chick pulmonary Wnt5a directs airway and vascular tubulogenesis. *Development*, *135* (7), 1365-1376. doi:10.1242/dev.010504

Lucas, P.C., O'Brien, R.M., Mitchell, J.A., Davis, C.M., Imai, E., Forman, B.M., Samuels, H.H., & Granner, D.K. (1991). A retinoic acid response element is part of a pleiotropic domain in the phosphoenolpyruvate carboxykinase gene. *Proc Natl Acad Sci U S A*, *88*(6), 2184-2188.

Maden, M. (2004). Retinoids in lung development and regeneration. *Curr Top Dev Biol*, *61*, 153-189. doi:10.1016/S0070-2153(04)61007-6

Maina, J.N. (2003). A systematic study of the development of the airway (bronchial) system of the avian lung from days 3 to 26 of embryogenesis: a transmission electron microscopic study on the domestic fowl, Gallus gallus variant domesticus. *Tissue cell*, *35*, 375-391. doi:10.1016/S0040-8166(03)00058-2

Maina, J.N. (2012). Comparative molecular developmental aspects of the mammalian- and the avian lungs, and the insectan tracheal system by branching morphogenesis: recent advances and future directions. *Front Zool*, *9*(1), 16. doi:10.1186/1742-9994-9-16

Malpel, S., Mendelsohn, C., &Cardoso, W.V. (2000). Regulation of retinoic acid signaling during lung morphogenesis. *Development*, *127*(14), 3057-3067.

Masin, M., Vazquez. J., Rossi, S., Groeneveld, S., Samson, N., Schwalie, P.C., Deplancke, B., Frawley, L.E., Gouttenoire, J., Moradpour, D., Oliver, T.G., &Meylan, E. (2015). GLUT3 is induced during epithelial-mesenchymal transition and promotes tumor cell proliferation in non-small cell lung cancer. *Cancer Metab*, *29*(2), 11. doi:10.1186/2049-3002-2-11

Massaro, G.D., & Massaro, D. (1996) Postnatal treatment with retinoic acid increases the number of pulmonary alveoli in rats. *Am J Physiol*, *270*(2 Pt 1), L305-10.

McInerney, E.M., Rose, D.W., Flynn, S.E., Westin, S., Mullen, T.M., Krones, A., Inostroza, J., Torchia, J., Nolte, R.T., Assa-Munt, N., Milburn, M.V., Glass, C.K., & Rosenfeld, M.G. (1998). Determinants of coactivator LXXLL motif specificity in nuclear receptor transcriptional activation. *Genes Dev*, *12*(21), 3357-3368.

Mentlein, R., & Heymann, E. (1987). Hydrolysis of retinyl esters by non-specific carboxylesterases from rat liver endoplasmic reticulum. *Biochem J*, *245*(3), 863-867.

Mercader, J., Madsen, L., Felipe, F., Palou, A., Kristiansen, K., & Bonet, M.L. (2007). All-trans retinoic acid increases oxidative metabolism in mature adipocytes. *Cell Physiol Biochem*, *20*(6), 1061-1072. doi:10.1159/0000110717

Metzger, R.J., Klein, O.D., Martin, G.R., & Krasnow, M.A. (2008). The branching programme of mouse lung development. *Nature*, *453*(7196), 745-750. doi:10.1038/nature07005

Metzler, M.A., & Sandell, L.L. (2016). Enzymatic Metabolism of Vitamin A in Developing Vertebrate Embryos. *Nutrients*, *8*(12), pii:E812. doi:10.3390/nu8120812

Mic, F.A., Haselbeck, R.J., Cuenca, A.E., & Duester, G. (2002). Novel retinoic acid generating activities in the neural tube and heart identified by conditional rescue of Raldh2 null mutant mice. *Development*, *129*(9), 2271-2282.

Montedonico, S., Sugimoto, K., Felle, P., Bannigan, J., & Puri, P. (2008) Prenatal treatment with retinoic acid promotes pulmonary alveologenesis in the nitrofen model of congenital diaphragmatic hernia. *J Pediatr Surg*, *43*(3), 500-507. doi:10.1016/j.jpedsurg.2007.10.030

Moore, T. (1937). Vitamin A and carotene: The vitamin A reserve of the adult human being in health and disease. *Biochem J*, *31*(1), 155-164.

Moriwaki, H., Blaner, W.S., Piantedosi, R., & Goodman, D.S. (1988). Effects of dietary retinoid and triglyceride on the lipid composition of rat liver stellate cells and stellate cell lipid droplets. *J Lipid Res*, *29*(11), 1523-1534.

Morrisey, E.E., & Hogan, B.L. (2010) Preparing for the first breath: genetic and cellular mechanisms in lung development. *Dev Cell*, *18*(1), 8-23. doi:10.1016/j.devcel.2009.12.010

Moura, R.S., Carvalho-Correia, E., daMota, P., & Correia-Pinto, J. (2014). Canonical Wnt Signaling Activity in Early Stages of Chick Lung Development. *PLoS ONE,* *9*(12), e112388. doi:10.1371/journal.pone.0112388

Moura, R.S., & Correia-Pinto, J. (2017). Molecular Aspects of Avian Lung Development. The Biology of the Avian Respiratory System. 129-146. Oxford: Academic Press. doi:10.1007/978-3-319-44153-5

Moura, R.S., Coutinho-Borges, J.P., Pacheco, A.P., daMota, P.O., & Correia-Pinto, J. (2011). FGF Signaling Pathway in the Developing Chick Lung: Expression and Inhibition Studies. *PLoS ONE*, *6*(3), e17660. doi:10.1371/journal.pone.0017660

Moura, R.S., Silva-Goncalves, C., Vaz-Cunha, P., & Correia- Pinto, J. (2016). Expression analysis of Shh signaling members in early stages of chick lung development. *Histochem Cell Biol*, *146*(4), 457-466. doi:10.1007/s00418- 016-1448-1

Moura, R.S., Vaz-Cunha, P., Silva-Gonçalves, C., & Correia-Pinto, J. (2015). Characterization of miRNA processing machinery in the embryonic chick lung. *Cell Tissue Res*, *362*(3), 569-575. doi:10.1007/s00441-015- 2240-6

Nagy, L., Kao, H.Y., Chakravarti, D., Lin, R.J., Hassig, C.A., Ayer, D.E., Schreiber, S.L., & Evans, R.M. (1997). Nuclear receptor repression mediated by a complex containing SMRT, mSin3A, and histone deacetylase. *Cell*, *89(*3), 373-380. doi:10.1016/S0092-8674(00)80218-4

Niederreither, K., Vermot, J., Messaddeq, N., Schuhbaur, B., Chambon, P., & Dolle, P. (2001). Embryonic retinoic acid synthesis is essential for heart morphogenesis in the mouse. *Development*, *128*(7), 1019-1031.

Nogueira-Silva, C., Carvalho-Dias, E., Piairo, P., Nunes, S., Baptista, M.J., Moura, R.S., & Correia- Pinto, J. (2011). Local Fetal Lung Renin-Angiotensin System as a Target to treat Congenital diaphragmatic hernia. *Mol Med*, *18*, 231-243. doi:10.2119/molmed.2011.00210

Noy, N., & Xu, Z.J. (1990). Thermodynamic parameters of the binding of retinol to binding proteins and to membranes. *Biochemistry*, *29*(16), 3888-3892.

O'Byrne, S.M., Wongsiriroj, N., Libien, J., Vogel, S., Goldberg, I.J., Baehr, W., Palczewski, K., & Blaner, W.S. (2005). Retinoid absorption and storage is impaired in mice lacking lecithin:retinol acyltransferase (LRAT). *J Biol Chem*, *280*(42), 35647-35657. doi:10.1074/jbc.M507924200

Oliveira, P.F., Martins, A.D., Moreira, A.C., Cheng, C.Y., & Alves, M.G. (2015) The Warburg effect revisited--lesson from the Sertoli cell. *Med Res Rev*, *35*(1), 126-151. doi:10.1002/med.21325

Ong, D.E. (1994). Cellular transport and metabolism of vitamin A: roles of the cellular retinoid-binding proteins. *Nutr Rev, 52*(2 Pt 2), S24-31.

Ornitz, D.M., & Yin, Y. (2012). Signaling Networks Regulating Development of the Lower Respiratory Tract. *Cold Spring Harb Perspect Biol*, *4*(5), pii: a008318. doi:10.1101/cshperspect.a008318

Pasutto, F., Sticht, H., Hammersen, G., Gillessen-Kaesbach, G., Fitzpatrick, D.R., Nurnberg, G., Brasch, F., Schirmer-Zimmermann, H., Tolmie, J.L., Chitayat, D., Houge, G., Fernandez-Martinez, L., Keating, S., Mortier, G., Hennekam, R.C., von der Wense, A., Slavotinek, A., Meinecke, P., Bitoun, P., Becker, C., Nurnberg, P., Reis, A., & Rauch, A. (2007). Mutations in STRA6 cause a broad spectrum of malformations including anophthalmia, congenital heart defects, diaphragmatic hernia, alveolar capillary dysplasia, lung hypoplasia, and mental retardation. *Am J Hum Genet*, *80*(3), 550-560. doi:10.1086/512203

Pereira-Terra, P., Moura, R.S., Nogueira-Silva, C., & Correia-Pinto, J. (2015). Neuroendocrine factors regulate retinoic acid receptors in normal and hypoplastic lung development. *J Physiol*, *593*(15), 3301-3311. doi:10.1113/JP270477

Pfaffl, M.W. (2001). A new mathematical model for relative quantification in real-time RT-PCR. *Nucleic Acids Res*, *29*(9), e45.

Quadro, L., Blaner, W.S., Salchow, D.J., Vogel, S., Piantedosi, R., Gouras, P., Freeman, S., Cosma, M.P., Colantuoni, V., & Gottesman, M.E. (1999). Impaired retinal function and vitamin A availability in mice lacking retinol-binding protein. *EMBO J*, *18*(17), 4633-4644. doi:10.1093/emboj/18.17.4633

Reboul, E., Berton, A., Moussa, M., Kreuzer, C., Crenon, I., & Borel, P. (2006). Pancreatic lipase and pancreatic lipase-related protein 2, but not pancreatic lipase-related protein 1, hydrolyze retinyl palmitate in physiological conditions. *Biochim Biophys Acta*, *1761*(1), 4-10. doi:10.1016/j.bbalip.2005.12.013

Ross, A.C., & Zolfaghari, R. (2011). Cytochrome P450s in the regulation of cellular retinoic acid metabolism. *Annu Rev Nutr*, *31*, 65-87. doi:10.1146/annurev-nutr-072610-145127

Ross, A.C., Zolfaghari, R., & Weisz, J. (2001) Vitamin A: recent advances in the biotransformation, transport, and metabolism of retinoids. *Curr Opin Gastroenterol*, *17*(2), 184-192.

Sakiyama, J., Yamagishi, A., & Kuroiwa, A. (2003). Tbx4-Fgf10 system controls lung bud formation during chicken embryonic development. *Development*, *130(7*), 1225-1234. doi:10.1242/dev.00345

Schmitz, H.H., Poor, C.L., Wellman, R.B., & Erdman, J.W.Jr. (1991). Concentrations of selected carotenoids and vitamin A in human liver, kidney and lung tissue. *J Nutr*, *121*(10), 1613-1621.

Schuger, L., Varani, J., Mitra, R. Jr., & Gilbride, K. (1993). Retinoic acid stimulates mouse lung development by a mechanism involving epithelial-mesenchymal interaction and regulation of epidermal growth factor receptors. *Dev Biol*, *159*(2), 462-473. doi:10.1006/dbio.1993.1256

Shih, M.Y., Kane, M.A., Zhou, P., Yen, C.L., Streeper, R.S., Napoli, J.L., & Farese, R.V.Jr. (2009). Retinol Esterification by DGAT1 Is Essential for Retinoid Homeostasis in Murine Skin. *J Biol Chem*, *284*(7), 4292-4299. doi:10.1074/jbc.M807503200

Singh, M., Singh, V.N., & Venkitasubramanian, T.A. (1968). Early effects of feeding excess vitamin A: hepatic glycogen, blood lactic acid, plasma NEFA and glucose tolerance in rats. *Life Sci*, *7*(5), 239-247.

So, E.N., & Crowe, D.L. (2000). Characterization of a retinoic acid responsive element in the human ets-1 promoter. *IUBMB Life*, *50*(6), 365-370. doi:10.1080/713803742

Tang, X.H., & Gudas, L.J. (2011). Retinoids, retinoic acid receptors, and cancer. *Annu Rev Pathol*, *6*, 345-364. doi:10.1146/annurev-pathol-011110-130303

Tierney, D.F. (1974). Lung metabolism and biochemistry. *Annu Rev Physiol*, *36*, 209-231. doi:10.1146/annurev.ph.36.030174.001233

Tourniaire, F., Musinovic, H., Gouranton, E., Astier, J., Marcotorchino, J., Arreguin, A., Bernot, D., Palou, A., Bonet, M.L., Ribot, J., & Landrier, J.F. (2015). All-trans retinoic acid induces oxidative phosphorylation and mitochondria biogenesis in adipocytes. *J Lipid Res*, *56*(6), 1100-1109. doi:10.1194/jlr.M053652

Tripathy, S., Chapman, J.D., Han, C.Y., Hogarth, C.A., Arnold, S.L., Onken, J., Kent, T., Goodlett, D.R., & Isoherranen, N. (2016). All-Trans-Retinoic Acid Enhances Mitochondrial Function in Models of Human Liver. *Mol Pharmacol*, *89*(5), 560-574. doi:10.1124/mol.116.103697

van Bennekum, A., Werder, M., Thuahnai, S.T., Han, C.H., Duong, P., Williams, D.L., Wettstein, P., Schulthess, G., Phillips, M.C., & Hauser, H. (2005) Class B scavenger receptor-mediated intestinal absorption of dietary beta-carotene and cholesterol. *Biochemistry*, *44*(11), 4517-4525. doi:10.1021/bi0484320

Veldhuizen, R., Nag, K., Orgeig, S., & Possmayer, F. (1998). The role of lipids in pulmonary surfactant. *Biochim Biophys* Acta, *1408*(2-3), 90-108. doi:10.1016/S0925-4439(98)00061-1

von Wichert, P. (1972). Studies on the metabolism of ischemic rabbit lungs. Conclusions for lung transplantation. *J Thorac Cardiovasc Surg*, *63*(2), 285-291.

Wagstaff, P., Kang, H.Y., Mylott, D., Robbins, P.J., & White, M.K. (1995) Characterization of the avian GLUT1 glucose transporter: differential regulation of GLUT1 and GLUT3 in chicken embryo fibroblasts. *Mol Biol Cell*, *6*(11), 1575-1589. doi:10.1091/mbc.6.11.1575

Warburton, D. (2008) Order in the lung. *Natur*e, *453*(7196), 733-735. doi:10.1038/453733a

Warburton, D., Bellusci, S., De Langhe, S., Del Moral, P.M., Fleury, V., Mailleux, A., Tefft, D., Unbekandt, M., Wang, K., & Shi, W. (2005). Molecular mechanisms of early lung specification and branching morphogenesis. *Pediatr Res*, *57*(5 Pt 2), 26R-37R. doi:10.1203/01.PDR.0000159570.01327.ED

Warburton, D., El-Hashash, A., Carraro, G., Tiozzo, C., Sala, F., Rogers, O., De Langhe, S., Kemp, P.J., Riccardi, D., Torday, J., Bellusci, S., Shi, W., Lubkin, S.R., & Jesudason, E. (2010). Lung organogenesis. *Curr Top Dev Biol*, *90*, 73-158. doi:10.1016/S0070-2153(10)90003-3

Wichterle, H., Lieberam, I., Porter, J.A., & Jessell, T.M. (2002). Directed differentiation of embryonic stem cells into motor neurons. *Cell*, *110*(3), 385-397.doi:10.1016/S0092-8674(02)00835-8

Wilson, L., Gale, E., & Maden, M. (2003). The role of retinoic acid in the morphogenesis of the neural tube. *J Anat*, *203*(4), 357-368. doi:10.1046/j.1469-7580.2003.00230.x

Wolf, G., Lane, M.D., & Johnson, B.C. (1957). Studies on the function of vitamin A in metabolism. *J Biol Chem*, *225*(2), 995-1008.

Yang, Q., Graham, T.E., Mody, N., Preitner, F., Peroni, O.D., Zabolotny, J.M., Kotani, K., Quadro, L., & Kahn, B.B. (2005) Serum retinol binding protein 4 contributes to insulin resistance in obesity and type 2 diabetes. *Nature*, *436*(7049), 356-362. doi:10.1038/nature03711

Yeager, H. Jr., & Massaro, D. (1972). Glucose metabolism and glyco-protein synthesis by lung slices. *J Appl Physiol*, *32*(4), 477-482.

Zachman, R.D. (1995). Role of vitamin A in lung development. *J Nutr*, *125*(6 Suppl), 1634S-1638S.